

**THE EFFECTS OF CYCLE-TO-CYCLE VARIATIONS ON NITRIC
OXIDE (NO) EMISSIONS FOR A SPARK-IGNITION ENGINE:
NUMERICAL RESULTS**

A Thesis

by

MILIVOY VILLARROEL

Submitted to the Office of Graduate Studies of
Texas A&M University
in partial fulfillment of the requirements for the degree of

MASTER OF SCIENCE

August 2004

Major Subject: Mechanical Engineering

**THE EFFECTS OF CYCLE-TO-CYCLE VARIATIONS ON NITRIC
OXIDE (NO) EMISSIONS FOR A SPARK-IGNITION ENGINE:
NUMERICAL RESULTS**

A Thesis

by

MILIVOY VILLARROEL

Submitted to Texas A&M University
in partial fulfillment of the requirements
for the degree of

MASTER OF SCIENCE

Approved as to style and content by:

Jerald A. Caton
(Chair of Committee)

Yassin A. Hassan
(Member)

Kalyan Annamalai
(Member)

Dennis O'Neal
(Head of Department)

August 2004

Major Subject: Mechanical Engineering

ABSTRACT

The Effects of Cycle-to-Cycle Variations on Nitric Oxide (NO) Emissions
for a Spark-Ignition Engine: Numerical Results. (August 2004)

Milivoy Villarroel, B.S., Virginia Polytechnic Institute and State University
Chair of Advisory Committee: Dr. Jerald A. Caton

The objectives of this study were to 1) determine the effects of cycle-to-cycle variations (ccv) on nitric oxide (NO) emissions, and 2) determine if the consideration of ccv affects the average NO emission as compared to the mean cycle NO emission. To carry out the proposed study, an engine simulation model was used. The simulation determines engine performance and NO emissions as functions of engine operating conditions, engine design parameters, and combustion parameters. An automotive, spark-ignition engine at part load and 1400 rpm was examined in this study. The engine cycle simulation employed three zones for the combustion process: (1) unburned gas, (2) adiabatic core region, and (3) boundary-layer gas. The use of the adiabatic core region has been shown to be especially necessary to capture the production of nitric oxides which are highly temperature dependent.

Past research has shown that cyclic variations in combustion cause ccv of burn duration, ignition delay and equivalence ratio. Furthermore, literature has shown that variations of these three input parameters may be approximated by a normal frequency distribution. Using the mean and standard deviation, and a random number generator, input values were tabulated for the ignition delay, burn duration and equivalence ratio. These three input parameters were then used to simulate cyclic variations in the combustion process.

Calculated results show that cyclic variations of the input parameters cause the cycle-by-cycle NO emissions to increase and decrease by as much as 59% from the mean cycle NO of 3,247 ppm. The average NO emission resulting from ccv was 4.9% less than the

mean cycle NO emission. This result indicates that cyclic variations must be considered when calculating the overall NO emissions.

DEDICATION

I would like to dedicate this thesis to my parents, Juan and Gregoria Villarroel, who have supported me unconditionally in my pursuit of a higher education. Also, my brother and sister for their advice and encouragement during my graduate studies.

ACKNOWLEDGEMENTS

I would like to express my gratitude to my advisor, Dr. Jerald A. Caton, for his support and guidance on my research project.

I would also like to thank Dr. Kalyan Annamalai and Dr. Yassin A. Hassan for serving on my thesis committee.

TABLE OF CONTENTS

| | Page |
|---|------|
| ABSTRACT..... | iii |
| DEDICATION..... | v |
| ACKNOWLEDGEMENTS..... | vi |
| TABLE OF CONTENTS..... | vii |
| LIST OF FIGURES..... | ix |
| LIST OF TABLES..... | xi |
| NOMENCLATURE..... | xii |
| CHAPTER | |
| I INTRODUCTION..... | 1 |
| II LITERATURE REVIEW..... | 3 |
| 2.1 Combustion Models..... | 3 |
| 2.2 Cyclic Variations in Combustion..... | 5 |
| 2.2.1 Fundamental Cause of ccv..... | 5 |
| 2.2.2 Factors Affecting ccv..... | 6 |
| III ENGINE SIMULATION MODEL..... | 10 |
| 3.1 Model Description..... | 10 |
| 3.2 Nitric Oxide Formation..... | 11 |
| IV ENGINE AND OPERATING SPECIFICATIONS..... | 14 |
| V CYCLE-TO-CYCLE MODELING..... | 15 |
| 5.1 Definitions..... | 15 |
| 5.2 Experimental Data..... | 15 |
| 5.3 Generating Input Data..... | 18 |
| VI RESULTS AND DISCUSSION..... | 20 |
| 6.1 Instantaneous NO Concentration..... | 20 |
| 6.2 Individual Effects on NO Formation..... | 21 |
| 6.2.1 Effect of Burn Duration on NO Formation..... | 21 |
| 6.2.2 Effect of Ignition Delay on NO Formation..... | 24 |
| 6.2.4 Effect of Equivalence Ratio on NO Formation..... | 25 |
| 6.3 Combined Effects on NO Formation..... | 27 |
| 6.3.1 Effect of Burn Duration and Ignition Delay on NO Formation... | 27 |

| CHAPTER | Page |
|--|------|
| 6.3.2 Effect of Burn Duration, Ignition Delay and Equivalence Ratio on NO Formation..... | 31 |
| 6.4 Coefficient of Variance of the Engine Performance Parameters..... | 34 |
| 6.5 Data Validation..... | 36 |
| VII SUMMARY AND CONCLUSION..... | 38 |
| 7.1 Summary..... | 38 |
| 7.2 Conclusion..... | 39 |
| REFERENCES..... | 40 |
| APPENDIX A..... | 42 |
| VITA..... | 45 |

LIST OF FIGURES

| | | Page |
|-------------|---|------|
| Figure 2-1 | Cyclic variation of flame shapes at 20° bTDC and TDC with a spark timing of 40° bTDC and 500 rpm..... | 7 |
| Figure 2-2 | Combustion chamber geometries..... | 9 |
| Figure 3-1 | Diagram of the three zones during combustion..... | 11 |
| Figure 5-1 | Mass fraction as a function of relative crank angle, with the data from Brehob and Newman [3] denoted for the various different time periods..... | 17 |
| Figure 5-2 | The normal frequency distribution for ignition delay with a mean and standard deviation of 12.5 and 1.44 CA, respectively..... | 19 |
| Figure 6-1 | Instantaneous nitric oxide concentration as a function of crank angle for the mean cycle..... | 21 |
| Figure 6-2 | The effect of combustion duration on NO formation..... | 22 |
| Figure 6-3 | Effect of combustion duration on maximum temperature and pressure.. | 23 |
| Figure 6-4 | Distribution of NO resulting from random variations of burn duration.. | 23 |
| Figure 6-5 | The effect of ignition delay on nitric oxide concentration..... | 24 |
| Figure 6-6 | Distribution of NO resulting from random variations of ignition delay.. | 25 |
| Figure 6-7 | The effect of equivalence ratio on NO and peak temperature..... | 26 |
| Figure 6-8 | Distribution of NO resulting from random variations of equivalence ratio..... | 27 |
| Figure 6-9 | Distribution of NO resulting from random variations of burn duration and ignition delay..... | 29 |
| Figure 6-10 | Average NO emissions as a function of simulation runs resulting from variations of burn duration and ignition delay..... | 29 |
| Figure 6-11 | Frequency distribution of NO resulting from 1,000 random variations of burn duration and ignition delay..... | 30 |
| Figure 6-12 | Distribution of NO resulting from random variations of burn duration, ignition delay and equivalence ratio | 31 |
| Figure 6-13 | Effect of equivalence ratio on brake specific fuel consumption..... | 32 |

| | Page |
|---|------|
| Figure 6-14 Average NO emissions as a function of simulation runs resulting from the simultaneous variations of all three input parameters..... | 33 |
| Figure 6-15 Frequency distribution of NO resulting from random variations of burn duration, ignition delay and equivalence ratio..... | 34 |
| Figure 6-16 Coefficient of variance for the various engine performance parameters. | 36 |
| Figure A-1 The effect of engine speed on NO formation..... | 43 |
| Figure A-2 The effect of spark timing on NO formation..... | 43 |
| Figure A-3 The effect of compression ratio on NO formation..... | 44 |
| Figure A-4 The effect of exhaust gas residual (EGR) on NO formation..... | 44 |

LIST OF TABLES

| | Page |
|--|------|
| Table 4-1 Engine input and other parameters..... | 14 |
| Table 5-1 Results for condition “A” from Brehob and Newman [3]..... | 16 |
| Table 5-2 Mean and standard deviation of the input parameters..... | 17 |
| Table 6-1 COV of the engine performance parameters due to individual variations of the input parameters..... | 35 |
| Table 6-2 Comparison of the mean and standard deviation of experimental data of Brehob and Newman [3] with that of the current simulation | 37 |

NOMENCLATURE

| | |
|----------------------|---|
| a | Weibe efficiency factor |
| AF | Air-fuel ratio |
| aTDC | After top dead center |
| BD | Burn duration |
| bTDC | Before top dead center |
| bsfc | Brake specific fuel consumption |
| CA | Crank angle (degrees) |
| COV | Coefficient of variance |
| ccv | Cycle-to-cycle variation |
| ER | Equivalence ratio |
| ID | Ignition delay |
| IMEP | Indicated mean effective pressure |
| k_i | Reaction rate constant for reaction i |
| m | Weibe form factor |
| NO | Nitric oxide |
| P_{peak} | Peak pressure |
| T_{peak} | Peak temperature |
| x_b | Mass fraction burned |
| σ | Standard deviation |
| θ | Crank angle |
| θ_b | Burn duration |
| θ_d | Ignition delay |
| θ_{pp} | Crank angle of peak pressure |
| θ_s | Start of combustion |
| ϕ | Equivalence ratio |
| μ | Mean |

CHAPTER I

INTRODUCTION

Over the years, there has been a great amount of work invested on research to improve the operation of internal combustion engines. After the invention of the computer, the field of computer modeling has flourished and has become a valuable tool for engineering analyzes. The use of simulation codes to model the thermodynamic cycle of an internal combustion engine has allowed for the development of cleaner, less noisy and more efficient engines for a variety of design and fuels. It allows for better understanding of the physicochemical phenomena and provides a platform for easy development and testing of new ideas [1]. With the advent of more powerful computers, modeling techniques have become very sophisticated and are widely used by designers. The engine models may not give exact results but they do give the designer the freedom to be innovative.

Engine simulations range from simple models that generate cylinder pressure and temperature diagrams to sophisticated models that are capable of predicting nitric oxide emissions. In general, the results obtained from simulation models agree with measured results acquired from experiments performed for the same conditions. Engine performance is influenced by many parameters and it would be time consuming to study the impact of each parameter on engine operation using physical prototypes. Using simulation models, various parameters can be varied and the results examined in a matter of seconds. This facilitates the study of thousands of cases in a short period of time. Also, engine simulations reduce the costs of the current experimental, trial and error approach used during the engineering design process.

This thesis follows the style and format of *Combustion and Flame*.

Currently, NO emissions can be modeled with reasonable accuracy for the conventional homogeneous-charge engine. In a homogeneous combustion process, liquid fuel is vaporized during the intake and compression process such that the vapor-air-exhaust gas mixture is evenly distributed throughout the combustion chamber. Most engine simulation models use average values for the combustion parameters and engine operating conditions when calculating engine performance parameters. These models are often referred to as mean cycle models. Although these models have good accuracy, they do not incorporate cyclic variations caused by combustion.

The stringent exhaust emission regulations have led to increased investigation on ways to reduce NO emissions. Cycle-to-cycle variations resulting from the inconsistency of the combustion process appear to cause higher engine emissions [2]. Results from literature [3, 4] show that cyclic variations in the combustion process causes ccv of burn duration, ignition delay and equivalence ratio. Furthermore, these variations can be approximated by a normal frequency distribution. The motivation for this study, therefore, was to determine the effects of ccv on nitric oxide emissions using an engine cycle simulation. Also, compare the average NO emission resulting from ccv with the mean cycle NO emission and determine if the mean cycle model can accurately predict the overall NO formation.

The first major chapter, Chapter II, presents a literature review. It summarizes the different combustion models that are currently being used in engine simulation models, followed by a discussion on the causes of cyclic variations in combustion. Chapter III gives an overview of the engine simulation model used for this study including details on the mechanism used for calculating nitric oxide concentration. In Chapter IV, the engine and operating specifications are given. A description of the input parameters and the technique used to simulate cyclic variations is presented in Chapter V. In Chapter VI, the results obtained from the various simulation experiments are presented. A summary of the results and the conclusion is given in Chapter VII.

CHAPTER II

LITERATURE REVIEW

2.1 Combustion Models

There are several mathematical models used to analyze the flow field and combustion process in spark-ignition engines. The mathematical models are divided into three groups: zero, quasi-, and multidimensional models. All three models can be used for estimating engine efficiency, performance and emissions.

In zero-dimensional models, the cylinder charge is assumed to be uniform in pressure, temperature and composition. Combustion chamber geometry and flame propagation is ignored for these models. Using the first law of thermodynamics, the pressure or heat release rate can be calculated. Depending on whether an experimentally determined pressure diagram or heat release rate is used, these models can be used as diagnostic (heat release analyzes) or predictive (pressure diagram analyzes) tools [1]. Most often, if the model is used as a predictive tool, the heat release or “burn fraction” rate is dictated by a Weibe function [5]

$$x_b(\theta) = 1 - \exp \left[-a \left(\frac{\theta - \theta_s}{\theta_b} \right)^{m+1} \right] \quad (2-1)$$

where the terms are:

θ = crank angle

θ_s = start of combustion

θ_b = burn duration

m = Weibe form factor

a = Weibe efficiency factor

The parameters a and n are adjustable parameters used to fit experimental data. Typically, $a=5$ and $m=2$.

Quasi-dimensional models take into consideration combustion flame propagation. As a result, the cylinder charge is divided into two zones: the burnt and unburnt gases. The two zones are separated by an infinitesimally thin flame front. The gases are assumed to be ideal gases where the burnt gases are assumed to be in chemical equilibrium and the unburnt gases are assumed to be frozen [1]. Also, the pressure is assumed to be uniform throughout the cylinder charge. Using the first law of thermodynamics, conservation of mass and volume, a system of first-order differential equations for the pressure, mass, volume and temperature of the burnt and unburnt gases are obtained.

The system of differential equations cannot be solved unless the burn rate is specified. Quasi-dimensional models try to predict the burn rate by assuming that the flame front propagates spherically through out the combustion chamber, and incorporating turbulence effects as an input. A more sophisticated approach considers the effects of turbulent length scales on flame propagation. A simplified form of the mass burning rate is given as [6]

$$\frac{dm_b}{dt} = \rho_u A_f U_t = \rho_u A_f ff U_1 \quad (2-2)$$

where the terms are:

ρ_u = density of the unburnt gas

A_f = area of the flame front

U_t = turbulent flame front velocity

ff = turbulent flame factor

U_1 = laminar flame front velocity

Multi-dimensional combustion models predict flame propagation by solving numerically the conservation equations of mass, linear momentum and energy in three dimensions [1]. These models typically use Computational Fluid Dynamics (CFD) codes to acquire the solution of the flow equations. Sub-models for processes such combustion and emissions are incorporated in the CFD programs. Because of the high computational demands, these models are mostly used for combustion chamber modeling rather than complete engine modeling [6].

2.2 Cyclic Variations in Combustion

Young [2], and Weaver and Santavicca [7] presented a study done by Soltau using high-speed movies of combustion. The results showed that cycle-to-cycle variations occur during the early stages of the combustion process, from the time of spark to the establishment of a fully developed flame. It is believed that early flame development can have a great effect on the combustion process. This is the period in which the developing flame kernel is susceptible to factors that cause ccv. In a study done by Starkman et al. [8], the reaction flame front histories were recorded for a modified CFR Supercharge Method engine. Flame arrival times were monitored by ionization gaps located along the centerline of the combustion chamber and in the direction of the flame travel. Results from four cycles showed that arrival time of the flame front at the first ionization gap varied by as much as 0.4 milliseconds from the average arrival time of 2 milliseconds.

2.2.1 Fundamental Cause of ccv

The fundamental cause of cycle-to-cycle variation in combustion is mainly due to cyclic variations of the turbulence level. Turbulence is generated as a result of the intake and compression processes, and the geometry of the combustion chamber. Young [2] reported that Soltau's high speed movies of flows in the combustion chamber showed that turbulent flow does not follow any pattern. Results show that turbulence increases the flame kernel growth which is caused by the turbulent wrinkling of the flame kernel

surface [9]. Wrinkling of the flame kernel increases the surface area which results in an increase in the mass burning rate. As a result, a faster initial flame growth will cause less cyclic variations in the flame growth.

Randomness of the flow as a result of turbulence also causes cyclic variations of the mean flow velocity near the spark plug at the time of ignition, which is believed to contribute to the cyclic variations in combustion [2]. Winsor and Patterson [10] studied combustion variations in a single-cylinder CFR (Cooperative Fuel Research) engine motored without fuel. Using a hot-wire anemometer, mixture velocities were measured for an engine speed of 1000 rpm. The results showed that the mixture velocity varied by as much as 6.5 ft/s for a resulting average value of 14.5 ft/s. According to Ozdor et al. [4], cyclic variations in the mean flow cause random convection that causes the flame kernel to be placed in different locations around the spark gap. The position of the flame center influences the flame front area which in turn directly affects the mass burning rate. As a result, the flame propagation in any cycle will differ. The closer is the flame kernel center to the center of the combustion chamber, the faster the burn is expected in the cycle.

2.2.2 Factors Affecting ccv

Studies have shown that variations of the local air-fuel ratio contribute to ccv in combustion. Brehob and Newman [3] reported that the air-fuel ratio of the gases varied at the spark plug gap with a standard deviation of 0.6 AF units. A decrease in AF ratio has been shown to increase the flame speed [11]. But, the increased flame speed did not increase the variations in flame speed, rather it lowered the deviations. Similarly, the equivalence ratio also varies from cycle to cycle and has been shown to effect early flame kernel growth. Ho and Santavicca [9] took measurements of the flame kernel size at the same time after ignition on an atmosphere pressure flow reactor. They found that the flame kernel size decreased as equivalence ratio lowered. Also, the relative variations in the flame kernel growth from one event to another increased with

decreasing equivalence ratio. These results are consistent with the results acquired by Bates [12], who used flame imagines to study ccv. Figure 2-1 shows the flame imagines taken at various cycles for an equivalency ratio of 0.75 and 0.9. At the higher equivalence ratio, there is less variation in the size and shape of the flames.

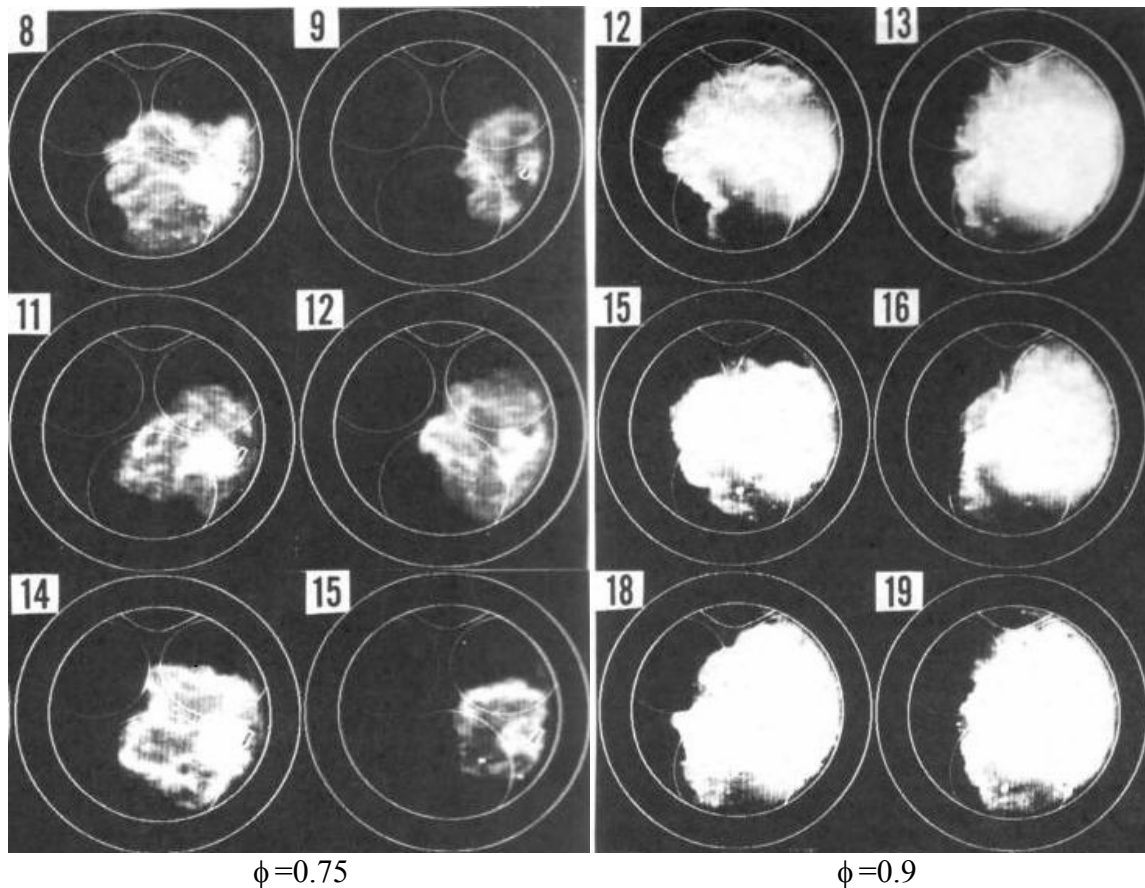


Fig. 2-1. Cyclic variation of flame shapes at 20° bTDC and TDC with a spark timing of 40° bTDC and 500 rpm [12].

As a result of imperfect scavenging there is always a residual gas remaining in the cylinder from a previous cycle. Weaver and Santavicca [7] performed tests on a single-cylinder CLR research engine with 0% and 10% nitrogen dilution. Results showed that dilution decreased the flame kernel radius by as much as 30% after ignition, and

increased the cyclic variations in combustion. They believed that dilution retards flame kernel growth due to lower flame speed and lower expansion velocity of the nitrogen diluted fuel/air mixture. The increased ccv in combustion is consistent with the generally accepted view that the higher the dilution, the less is the burning rate, and the greater the ccv in engine performance [4]. Also, charge dilution by air or exhaust gas causes the combustion duration and ignition delay to increase.

Barton et al. [11] have shown that engine speed significantly affects the magnitude of combustion variations. In a study conducted on a CFR-RDH engine, data from more than 200 cycles was collected for various sets of conditions. The results showed that the average flame speed and cyclic flame speed variations increased by increasing the engine speed. The increase in combustion variations appear to be due primarily to increases in the mixture motion variations. Turbulence also appears to increase with increased engine speed and the higher turbulence is believed to be the cause for the increase in flame speed variations [2].

Heywood and Vilchis [13] showed that fuel type influences cyclic variations during combustion, especially during the initially flame kernel development. In a study, they compared the size and shape of the flame in a combustion chamber of a single cylinder engine with a square cross-section. Propane and hydrogen were used as fuels. The schlieren photographic technique was used to visualize and record the process. The photographs showed that the size and shape of the hydrogen flame repeated closely from cycle to cycle, and the flame remained centered at the spark plug electrodes. On the other hand, pictures of the propane flame showed substantial variations from cycle to cycle. Also, the flame growth of the hydrogen-air mixture was much quicker. The higher burning rate is believed to reduce the effect of the mean in-cylinder motion, resulting in small cyclic variations of the flame location [4, 13].

Combustion chamber design has been studied and results show that it too influences cyclic variations in combustion. Lucas and Brunt [14] investigated the effects of chamber design using a disc chamber geometry and various squish type chambers that included a bathtub and bowl-in-piston design with a squish area of 48% and 47%, respectively. Figure 2-2 shows the two types of chamber geometries. The disc chamber with side ignition was used as reference to allow quantitative comparison of the performance and combustion parameters obtained with different chambers. Experimental results showed that the bathtub design had the largest decrease in cyclic variations with 50% and a 12.2% reduction in burn duration. This might be due to the fact that increasing the squish area will yield high flame areas. The effect of the spark plug location was also examined using the disc chamber [14]. The spark plug was moved from its original position at a radius of 19 mm to the centre of the chamber. The central spark plug location decreased the cyclic dispersion by 13.6% and the burn duration by 6.9%. In a similar study, Heywood and Poulus [15] showed that moving the spark plug to the centre resulted in increased flame area. These results indicate a decrease in cyclic variations for combustion chambers with high burning rates.

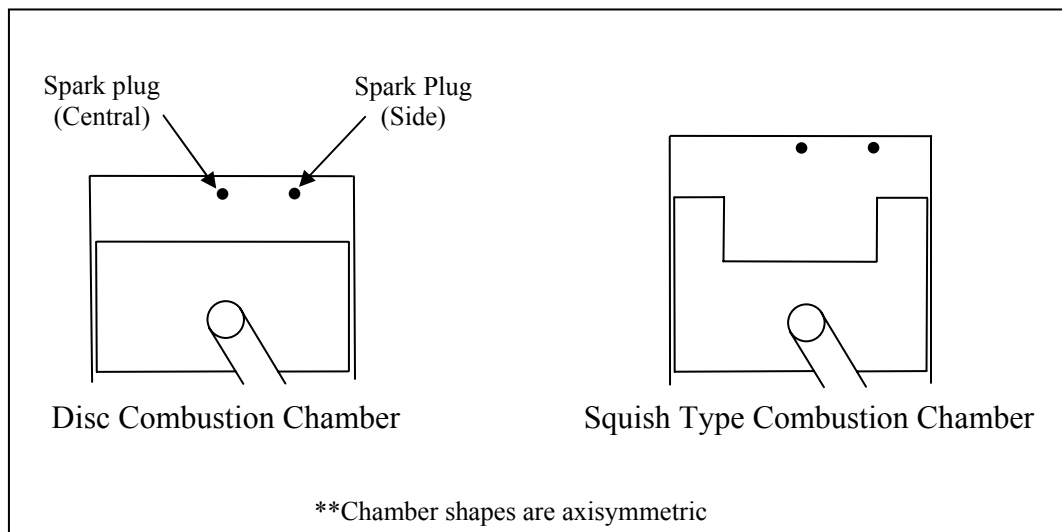


Fig. 2-2. Combustion chamber geometries.

CHAPTER III

ENGINE SIMULATION MODEL

An engine cycle simulation was used to predict the effects of cycle-to-cycle variation on nitric oxide emissions. The simulation determines engine performance and NO emissions as functions of engine operating conditions, engine design parameters, and combustion parameters. A complete description of the simulation model can be found elsewhere [16-19]. Some of the important features of the model will be discussed in this chapter.

3.1 Model Description

The simulation uses variable thermodynamic gas properties to model a four-stroke cycle, spark-ignition engine. It captures the important features of the four-stroke cycle including the intake, compression, combustion, expansion and exhaust process. The cylinder contents during the compression, expansion and exhaust processes occupy one zone. The exhaust process occupies two zones, one for the fresh charge and the other for the residual gases. For the combustion process, the engine cycle simulation employed three zones: (1) unburned gas, (2) adiabatic core region, and (3) boundary-layer gas. The high temperature adiabatic core and the lower temperature thermal boundary layer makeup the burned region as shown in Figure 3-1. The use of the adiabatic core region has been shown to be especially necessary to capture the production of nitric oxides which are highly temperature dependent. During all processes, each zone is assumed to be spatially homogeneous. The combustion process is dictated by the Wiebe function [5] which represents the mass fraction of fuel burned.

The instantaneous gas temperature, cylinder pressure, volume and mass, vary only as a function of time (crank angle). Using the first law of thermodynamics, governing differential equations for the parameters mentioned above were derived for the one-zone,

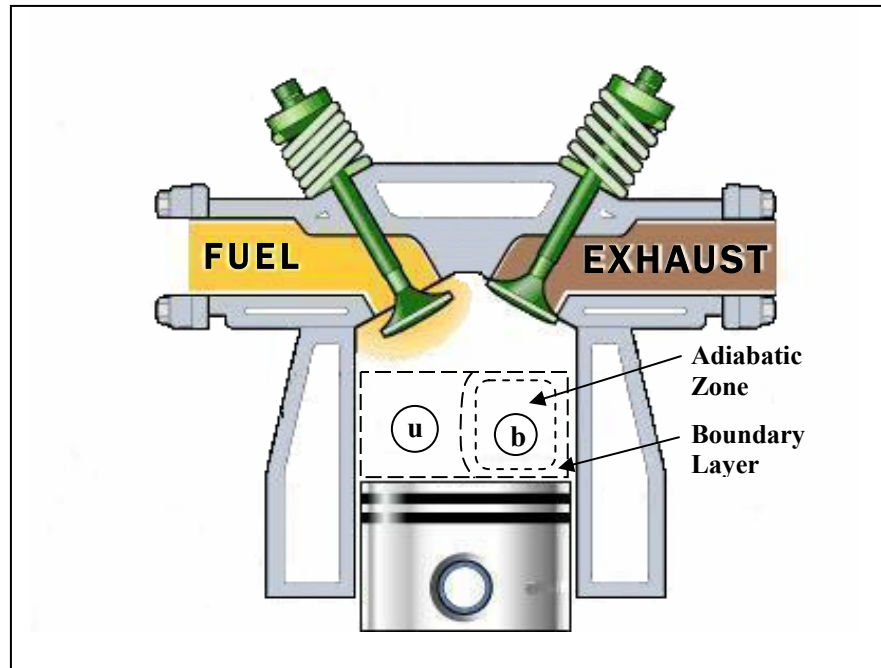


Fig. 3-1. Diagram of the three zones during combustion.

two-zone and three-zone systems. The equations cannot be solved analytically, so the Euler technique was used to solve these differential equations numerically, which yielded results similar to the Runge-Kutta method. For each cycle, the initial amount of exhaust gases (residual), and the initial gas temperature and pressure are assumed. The complete calculation is repeated until the initial values converge with the final values. Usually it takes less than three iterations to converge.

3.2 Nitric Oxide Formation

The formation of nitrogen oxides (NO_x) result from the reaction of atomic oxygen and nitrogen during the combustion process [5]. Nitric oxide (NO) is the most dominant component of NO_x , with nitric dioxide (NO_2) making up only 1% to 2% of the total NO_x . NO is highly temperature dependent and is formed in the high temperature (typically above 1800 K) burned gases behind the flame front [6].

To calculate the nitric oxide concentration, the extended Zeldovich mechanism was used [20]. The reaction steps are as follows,



where k_1 , k_2 and k_3 are the reaction rate constants as a consequence of chemical forces driving the reaction. Using the law of stoichiometry or law of mass action, the overall nitric oxide formation rate can be derived. To carry out this derivation, two assumptions are made. The nitrogen atoms are assumed to be in steady state since the concentration of N atoms is very small. Equilibrium conditions are assumed for the other species (such as N_2 , O_2 , OH , H and O) because at high pressures and temperatures in spark-ignition engines, the hydrocarbon oxidation reactions go rapidly to completion [21]. For these conditions, the nitric oxide formation is governed by the following equation [22],

$$\frac{d[\text{NO}]}{dt} = \frac{2R_1(1-\beta^2)}{(1+\beta K)} \quad (3-4)$$

where the terms are:

$$R_1 = k_1^+ [\text{O}]_e [\text{N}_2]_e = k_1^- [\text{NO}]_e [\text{N}]_e \quad (3-5)$$

$$R_2 = k_2^+ [\text{N}]_e [\text{O}_2]_e = k_2^- [\text{NO}]_e [\text{O}]_e \quad (3-6)$$

$$R_3 = k_3^+ [\text{N}]_e [\text{OH}]_e = k_3^- [\text{NO}]_e [\text{H}]_e \quad (3-7)$$

$$\beta = \frac{[\text{NO}]}{[\text{NO}]_e} \quad (3-8)$$

$$K = \frac{R_1}{R_2 + R_3} \quad (3-9)$$

where the brackets denote molal concentration in kmole/m^3 , k_i^+ and k_i^- are the forward and backward reaction rate constant for reaction i , respectively, R_i is the reaction rate for reaction i , and β is the ratio of the nitric oxide concentration to its equilibrium value. To calculate the instantaneous nitric oxide concentration, the NO formation rate is multiplied by the instantaneous adiabatic zone volume and the time elapsed. For this study, the nitric oxide kinetics recommended by Dean and Bozzelli [23] were used.

CHAPTER IV

ENGINE AND OPERATING SPECIFICATIONS

For this study a 5.7L, V-8 automotive spark-ignition engine operating at part load and at 1400 rpm with a compression ratio of 8.1:1 was examined. The complete specification of the engine is given elsewhere [24]. A sample of the input parameters required for the simulation model is listed in Table 4-1. The choice of values for the burn duration and ignition delay will be discussed in the next chapter. All other values represent average values acquired from experimental data. Running the engine simulation with the corresponding values will yield the mean cycle engine performance parameters.

Table 4-1
Engine input and other parameters

| | |
|--------------------------|-----------|
| Fuel | isooctane |
| AF (Stoichiometric) | 15.13 |
| Frictional MEP (kPa) | 72.4 |
| Inlet Pressure (kPa) | 51.4 |
| Exhaust Pressure (kPa) | 105 |
| Engine Speed (rpm) | 1400 |
| Inlet Temperature (K) | 319 |
| Cylinder Wall Temp (K) | 450 |
| Fuel LHV (kJ/kg) | 44,400 |
| Combustion Duration (CA) | 45 |
| Spark Timing (CA) | -26.5 |
| Ignition Delay (CA) | 12.5 |
| "Switch" Temperature (K) | 1200 |
| "Step" Size (CA) | 0.25 |
| Combustion Parameters: | |
| m= | 2 |
| a= | 5 |

CHAPTER V

CYCLE-TO-CYCLE MODELING

To simulate cycle-to-cycle variations of the proposed engine, one or more of the input parameters were changed at the beginning of each run. For this study, the combustion duration, ignition delay and equivalence ratio were varied since they have been shown to be greatly affected by cyclic variations in combustion. The final operating conditions at the end of each run were not carried over as the initial operating conditions for the next run. In this way, many individual cycles were simulated that represent cyclic variations.

5.1 Definitions

For this simulation study, the following definitions will be used. Ignition delay, θ_d , is defined as the crank angle (degrees) interval between the time of spark firing and the start of combustion. Combustion duration, θ_b , is the number of crank angle degrees required to completely burn the air-fuel mixture. In some cases ignition delay and combustion duration are defined as the crank angle degrees to burn 2% and 90% of the air-fuel mixture, respectively. The equivalence ratio, ϕ , is defined as the stoichiometric air-fuel ratio divided by the actual air-fuel ratio [5]:

$$\phi = \frac{(A : F)_{\text{Stoich}}}{A : F} \quad (5-1)$$

The mixture is called stoichiometric if $\phi = 1$, lean if $\phi < 1$, and rich if $\phi > 1$.

5.2 Experimental Data

Results from literature show that cyclic variations of combustion duration, ignition delay and equivalence ratio may be approximated by a normal frequency distribution. The work of Brehob and Newman [3] has been used to approximate the mean and standard

deviation for combustion duration and ignition delay. In the study, experimental data was obtained using a Ricardo Hydra, single-cylinder, spark-ignition engine. They presented results from 500 consecutive, individual cycles. Their results included the mean and standard deviation of several burn durations, peak cylinder pressures, crank angles of peak pressure, and indicated mean effective pressures. For the most part, the results were consistent with a normal distribution. Table 5-1 is a summary of their results for one engine operating condition.

Table 5-1

Results for condition “A” from Brehob and Newman [3]

| Item | Mean Value | Standard Deviation |
|----------------------|-------------------|---------------------------|
| Burn Duration: | | |
| 0 – 2% | 19.7 CA | 1.44 CA |
| 0 – 10% | 25.8 CA | 1.63 CA |
| 0 – 90% | 47.3 CA | 3.26 CA |
| 10 – 90% | 21.5 CA | 2.06 CA |
| | | |
| p_{peak} | 21.0 bar | 1.47 bar |
| θ_{pp} | 16.3 aTDC | 1.91 CA |
| IMEP | 4.12 bar | 0.037 bar |

To compare the performance parameters measured by Brehob and Newman [3] with that of the current simulation, a conversion was needed to obtain the complete burn duration (0–100%) which is used in the current work. This conversion yielded an ignition delay (ignition – 0%) of 12.5 CA, and burn duration (0–100%) of 45.0 CA. A comparison of these results is shown in Figure 5-1. The fit of the data from Brehob and Newman [3] to the burn curve used in the current work is good.

Table 5-2 shows a summary of the mean and standard deviation for each input parameter that was varied in this study. Since the proposed engine is operating at stoichiometric conditions, an average equivalence ratio of 1.0 with a corresponding standard deviation of 0.038 was used. The standard deviation was derived from the results reported by

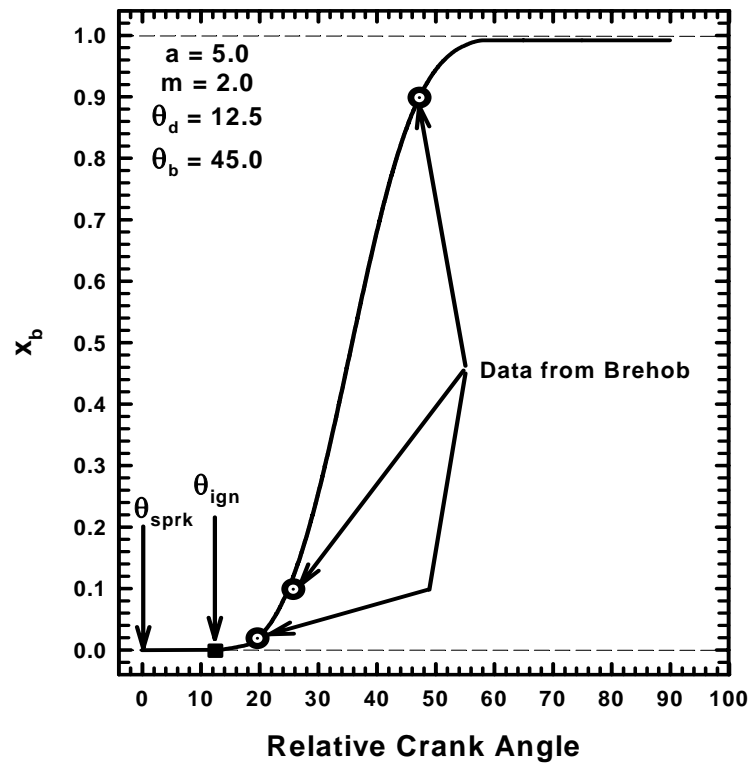


Fig. 5-1. Mass fraction burned as a function of relative crank angle, with the data from Brehob and Newman [3] denoted for the various different time periods.

Brehob and Newman [3]. The standard deviation for the ignition delay and combustion duration were approximated by the experimental values corresponding to a burn duration of 0-2% and 0-90%, respectively.

Table 5-2

Mean and standard deviation of the input parameters

| | Combustion Duration (CA) | Ignition Delay (CA) | Equivalence Ratio |
|----------------|--------------------------|---------------------|-------------------|
| Mean | 45 | 12.5 | 1.0 |
| Std. Deviation | 3.26 | 1.44 | 0.038 |

5.3 Generating Input Data

The input values for the burn duration, ignition delay and equivalence ratio were generated using a random number generator such that the distribution follows the empirical rule. The "empirical rule" states that for a normal distribution about 68% of the sample data falls within one standard deviation of the mean, 95% falls within two standard deviations, and 99.7% falls within three standard deviations of the mean. Thus, almost all values lie within 3 standard deviations of the mean. For the case of the ignition delay with a mean and standard deviation of 12.5 CA and 1.44 CA, respectively;

68% of the values fall approximately between 11.1 and 13.9 CA

95% of the values fall approximately between 9.6 and 15.4 CA

99.7 % of the values fall approximately between 8.2 and 16.8 CA

A normal density curve along with the relative distribution was created for the ignition delay as shown in Figure 5-2. A similar approach was used to tabulate the input values for the burn duration and equivalence ratio. The normal frequency distribution is defined as

$$f(x) = \frac{1}{\sigma\sqrt{2\pi}} e^{-\frac{(x-\mu)^2}{2\sigma^2}} \quad (5-2)$$

where σ is the standard deviation and μ is the mean.

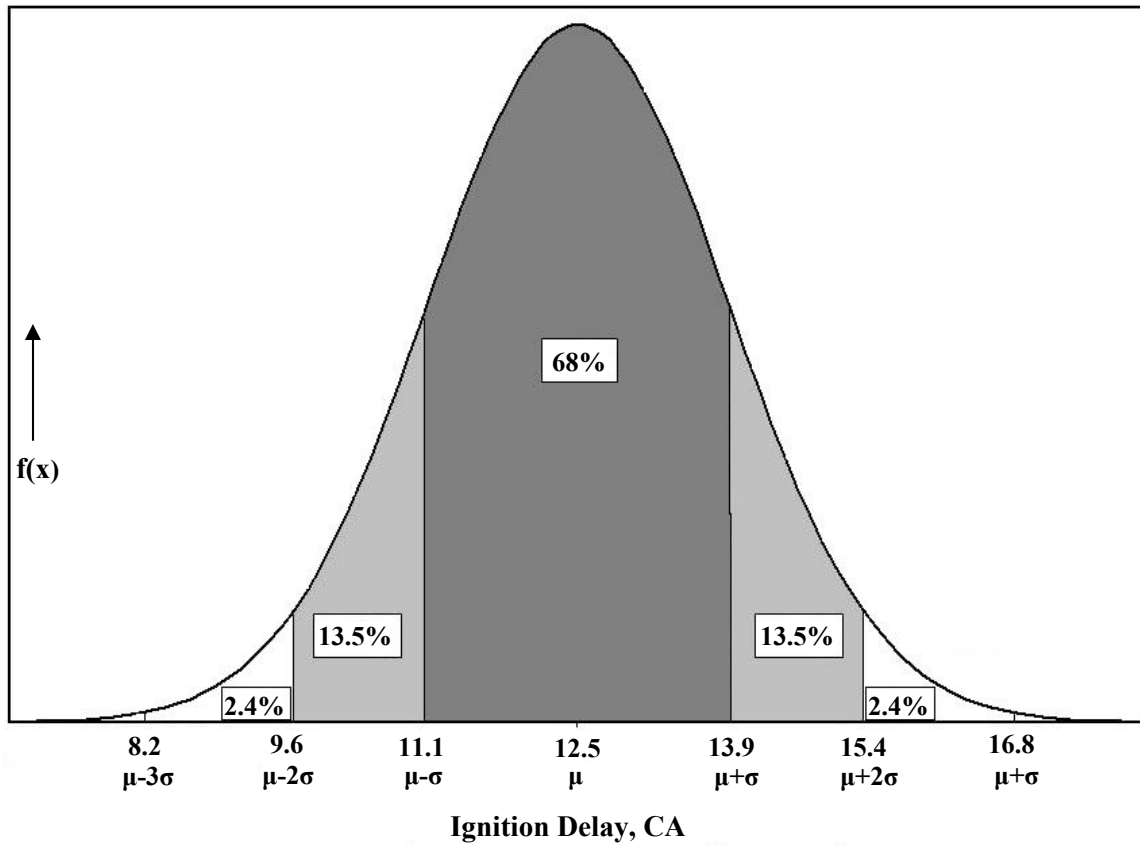


Fig. 5-2. The normal frequency distribution for ignition delay with a mean and standard deviation of 12.5 and 1.44 CA, respectively.

CHAPTER VI

RESULTS AND DISCUSSION

In this study, the engine simulation model calculated the cycle-to-cycle variations of nitric oxide concentration, maximum cylinder temperature and pressure, crank angle of peak pressure, brake specific fuel consumption (bsfc) and indicated mean effective pressure (IMEP). The variation of NO emissions resulting from cyclic variations of burn duration, ignition delay or equivalence ratio will be examined first. This way, the effect of each parameter on the formation of NO can be analyzed. Next, two parameters (burn duration and ignition delay) will be varied simultaneously and the variations of NO will be calculated. Then, the effect of varying all three input parameters simultaneously will be examined. For each case, the percent variation of NO from the mean cycle NO will be calculated. Also, the coefficient of variance for the input and performance parameters will be tabulated to measure the variability and sensitivity of each parameter.

6.1 Instantaneous NO Concentration

The instantaneous nitric oxide concentration as a function of crank angle for the mean cycle is shown in Figure 6-1. The details of the NO computations are provided elsewhere [16]. Ignition occurs at 26.5° bTDC, but nothing happens until combustion begins at 14° bTDC. This results in an ignition delay of 12.5 CA. At the beginning of combustion, the formation of NO starts off slowly but then increases rapidly from TDC until it reaches a maximum at the end of combustion (31° aTDC). The total NO is composed of the nitric oxide in the adiabatic zone and the boundary layer. The amount of nitric oxide transported into the boundary layer is removed from the adiabatic zone. When the temperature of the burned gases falls to about 2000 K, the reaction rates are relatively low and the composition of the products including NO do not change much with further cooling [6]. From Figure 6-1, the total NO concentration for the mean cycle is 3,247 ppm.

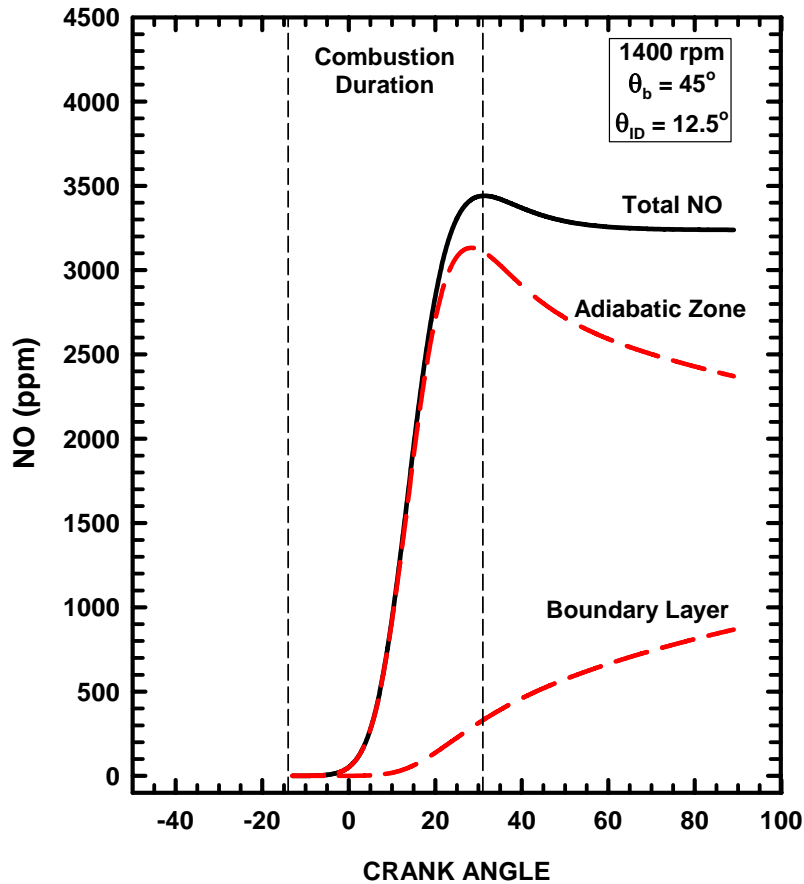


Fig. 6-1. Instantaneous nitric oxide concentration as a function of crank angle for the mean cycle.

6.2 Individual Effects on NO Formation

In this section the individual effects of burn duration, ignition delay and equivalence ratio on NO concentration will be examined. As mentioned before, each parameter was varied for a range of values that are within three standard deviations of its mean. When simulating cyclic variations, the selected number of input values satisfied the empirical rule.

6.2.1 Effect of Burn Duration on NO Formation

Figure 6-2 shows the effect of burn duration on nitric oxide concentration. It is evident from the plot that the formation of NO decreases almost linearly as combustion duration

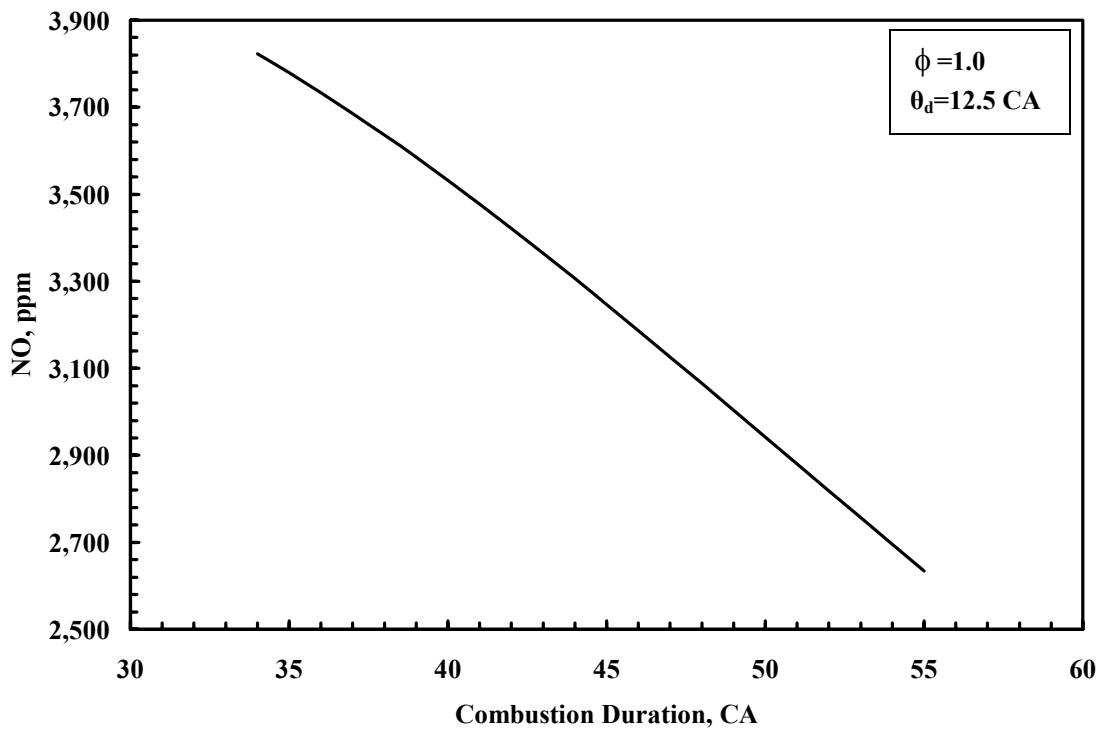


Fig. 6-2. The effect of combustion duration on NO concentration.

increases. This occurs because an increase in burn duration decreases the maximum temperature and pressure in the cylinder as shown in Figure 6-3. As a result, the NO concentration also decreases.

The distribution of NO resulting from 200 random cyclic variations of burn duration is presented in Figure 6-4. For this case, the ignition delay and equivalence ratio were kept constant at the average value of 12.5 CA and 1.0, respectively. The cyclic dispersions caused the exhaust NO emission to increase and decrease by as much as 18% with a maximum and minimum value of 3,812 ppm and 2,680 ppm, respectively. The average NO resulting from the ccv was 3,239 ppm, a difference of less than 0.5% from the mean cycle NO of 3,247 ppm. From this result, it can be concluded that cyclic variations of combustion duration alone has a minimal effect on the overall NO concentration.

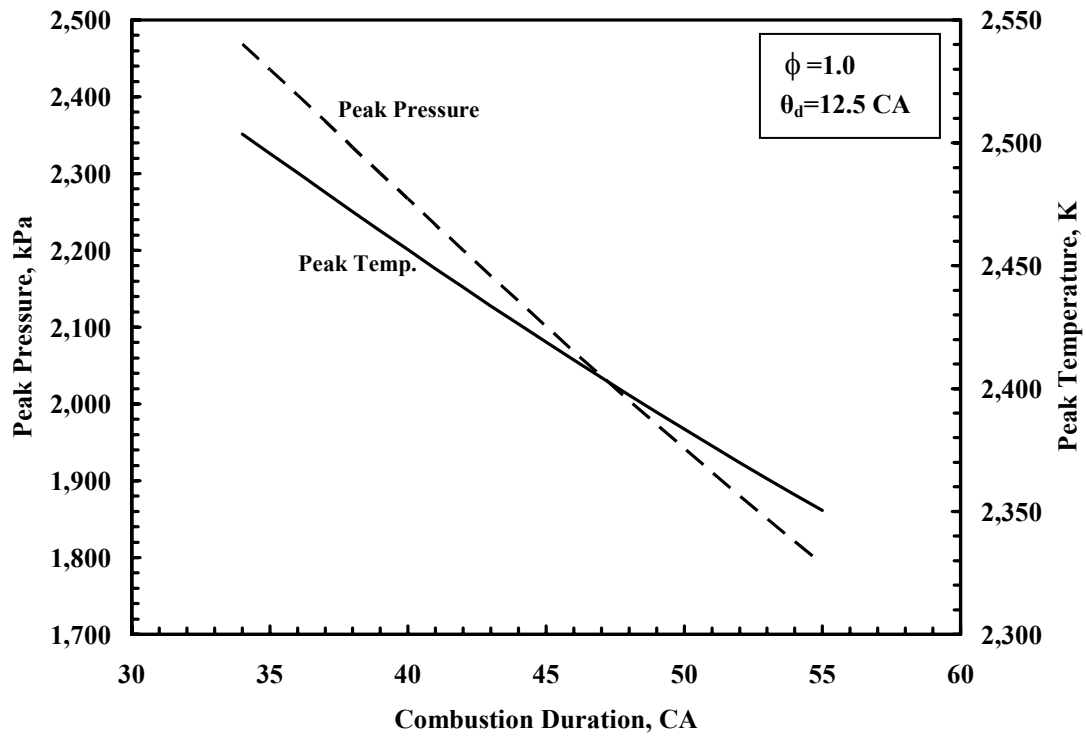


Fig. 6-3. Effect of combustion duration on maximum temperature and pressure.

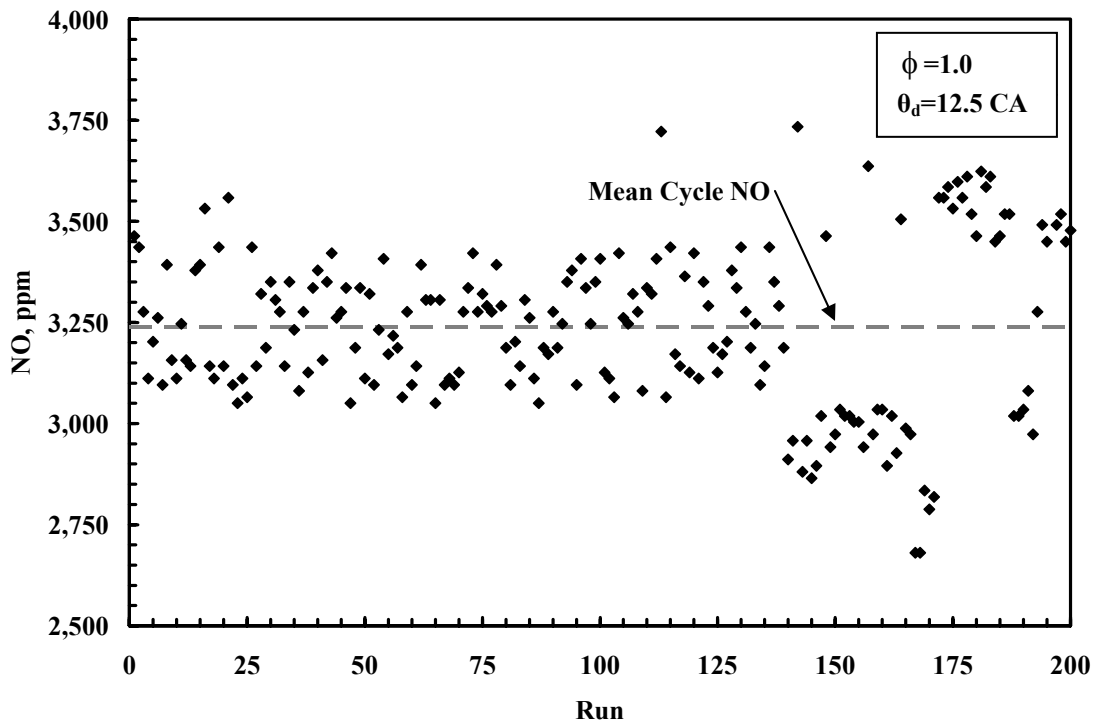


Fig. 6-4. Distribution of NO resulting from random variations of burn duration.

6.2.2 Effect of Ignition Delay on NO Formation

Figure 6-5 presents the effect of ignition delay on NO emissions. The NO concentration decreases linearly with increasing ignition delay. Again, an increase in ignition delay causes the peak temperature and pressure in the cylinder to decrease and as a result the NO formation decreases. With this result, it can be expected that maximum NO emissions will occur when ignition delay and burn duration are both small.

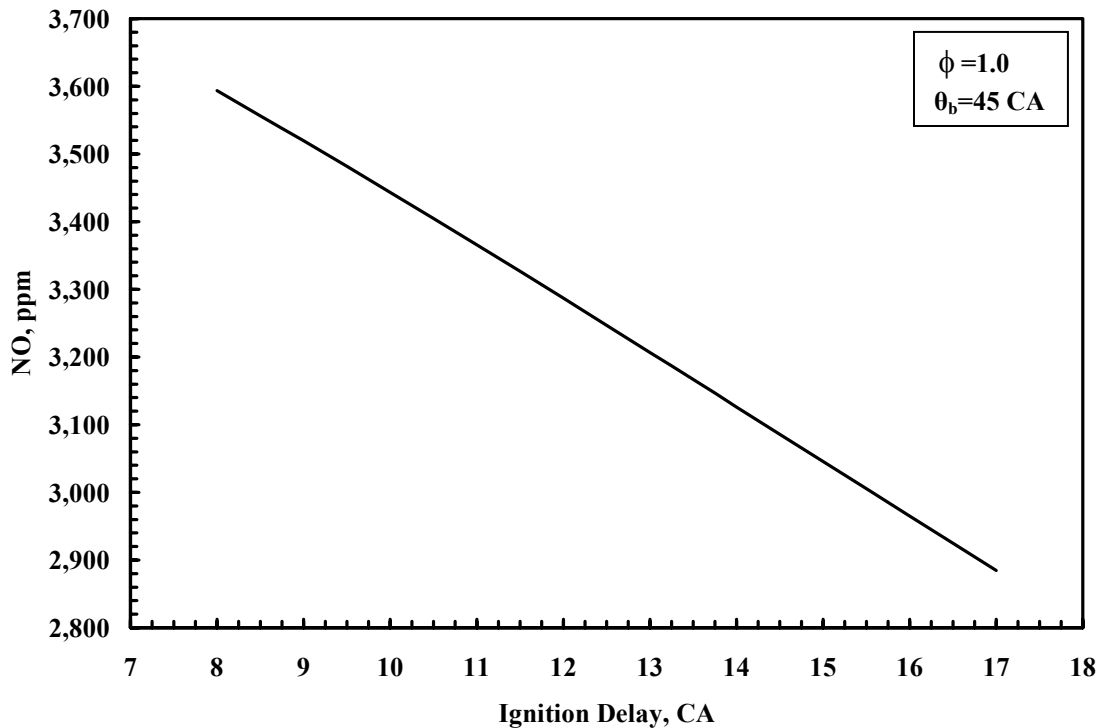


Fig. 6-5. The effect of ignition delay on nitric oxide concentration.

The results obtained from 200 random variations of ignition delay are shown in Figure 6-6. The ccv caused the NO concentration to fluctuate by as much as 10% for each run with a maximum and minimum value of 3,575 ppm and 2,985 ppm, respectively. The average NO emission resulting from the cyclic variations was found to be 3,245 ppm. The difference between the average NO resulting from ccv and the mean cycle NO is less than 0.1%. Therefore, ccv of ignition delay alone has almost no effect on the overall formation of exhaust NO emissions.

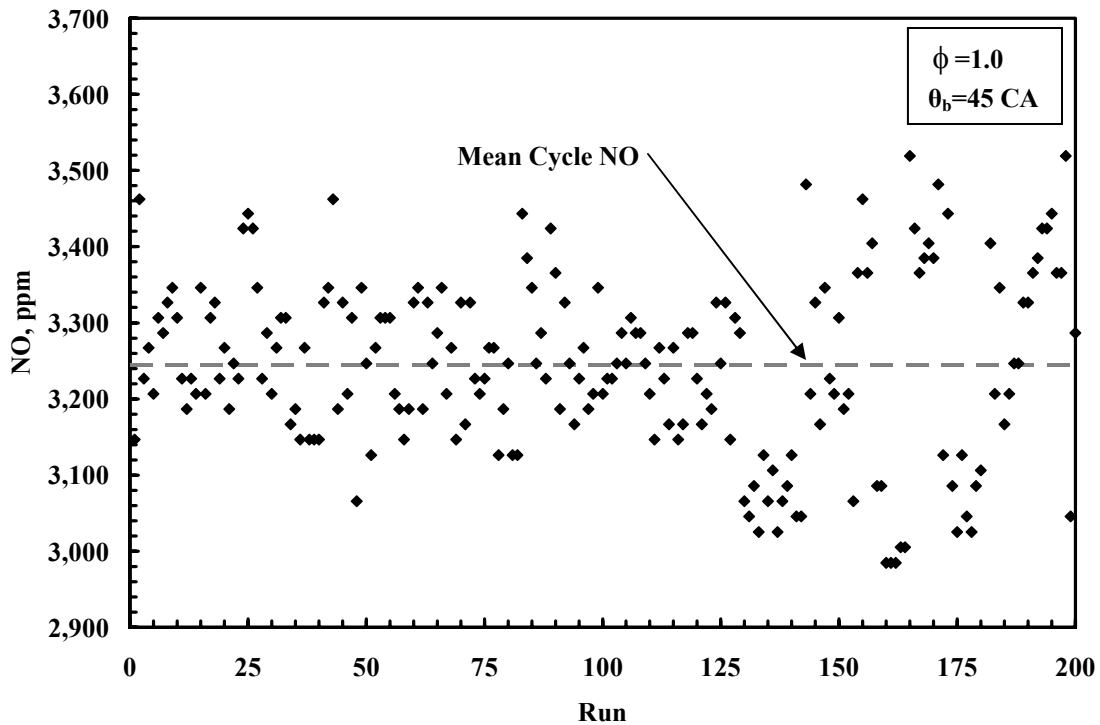


Fig. 6-6. Distribution of NO resulting from random variations of ignition delay.

6.2.3 Effect of Equivalence Ratio on NO Formation

The effect of equivalence ratio on NO emissions and peak temperature is shown in Figure 6-7. The plot shows that the highest nitric oxide concentration results for slightly lean mixtures with an equivalence ratio of about 0.94. As mentioned before, NO formation is strongly favored with increasing temperature. According to the figure, maximum NO formation should occur at slightly rich ($\phi \sim 1.05$) where burned gas temperatures are maximized. But, in slightly rich mixtures there is a decreased amount of NO concentration due to the decreasing oxygen concentration in the burned gases. Studies have shown that oxygen availability is the second most dominant variable in NO formation.

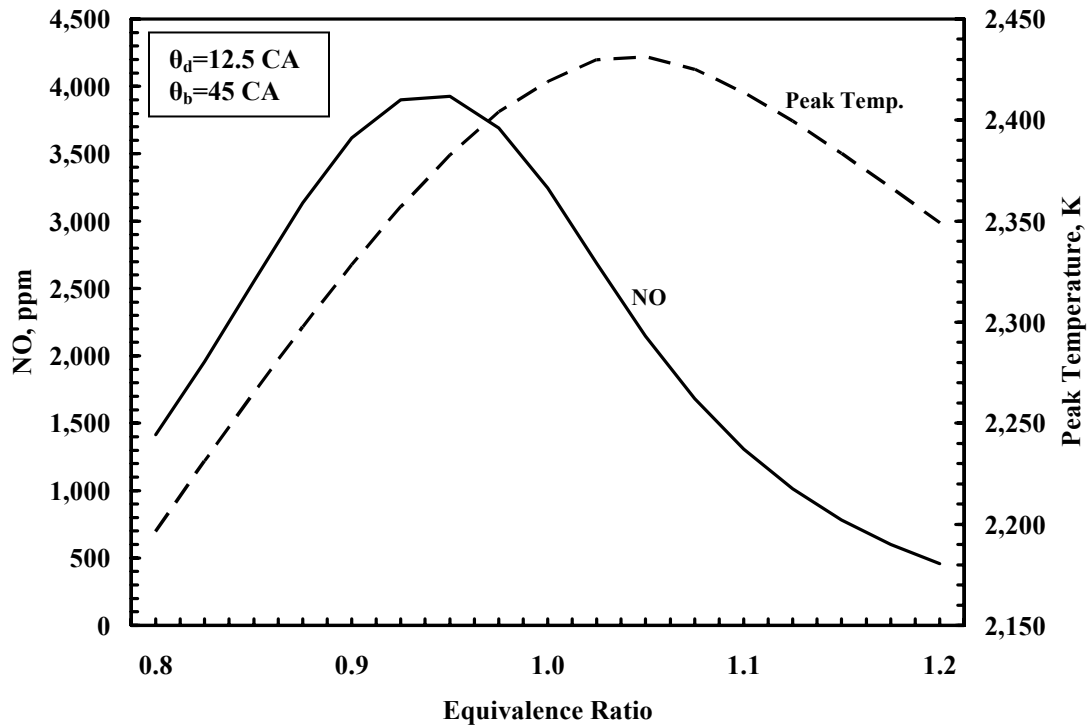


Fig. 6-7. The effect of equivalence ratio on NO and peak temperature.

At slightly lean mixtures, there is a slight excess of oxygen atoms that can react with the nitrogen atoms to form nitric oxide. Also, the rate of NO formation is a maximum near stoichiometric conditions. As a result, maximum NO occurs at just below stoichiometric. For $\phi \leq 0.9$ and $\phi \geq 1.1$, the temperature dominates the NO formation which decreases as the temperature falls. Figure 6-7 indicates that NO formation will be negligible for $\phi \leq 0.7$, since the gas temperature appears to drop quickly and will be sufficiently low.

The distribution of NO resulting from 200 random variations of equivalence ratio is shown in Figure 6-8. The ccv caused the NO concentration to fluctuate by as much as 59% for each run with a maximum and minimum value of 3,947 ppm and 1,321 ppm, respectively. The average NO emission was found to be 3,108 ppm, a reduction in NO emissions of 4.3% as compared to the mean cycle NO. The reason for this is that the NO concentration is reduced for a large fraction of the operating range as shown in Figure 6-7.

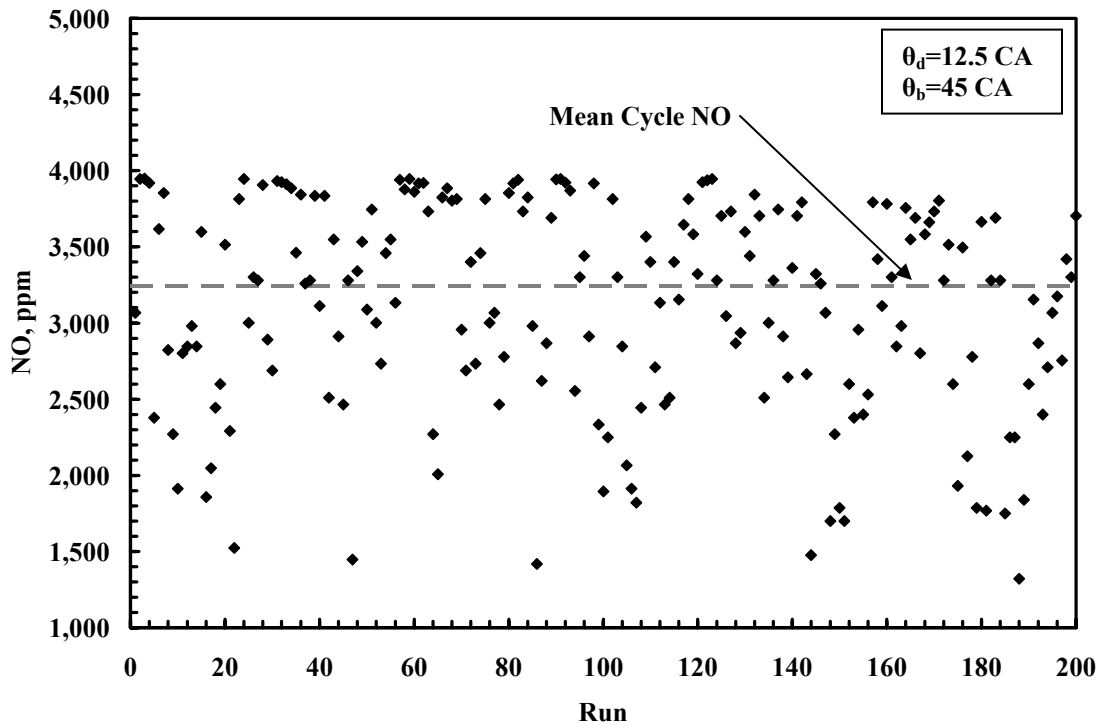


Fig. 6-8. Distribution of NO resulting from random variations of equivalence ratio.

6.3 Combined Effects on NO Formation

The effects of varying the input parameters simultaneously will now be examined. First, only burn duration and ignition delay were varied. Second, all three parameters were varied. For each case the results are reported and a frequency distribution was plotted to determine if the variations of NO can be approximated by a normal distribution. Also, a calculation of the number of runs or cycles required to reach a fairly constant average NO value will be presented.

6.3.1 Effect of Burn Duration and Ignition Delay on NO Formation

The effect of varying both the combustion duration and ignition delay simultaneously will now be examined. For this part of the study, 1,000 random combinations of both parameters will be employed and the NO calculated. From the previous results it is expected that the maximum and minimum possible NO concentration are 4,056 ppm and

2,278 ppm, respectively. The maximum will occur for an ignition delay and burn duration of 8 and 34 CA, respectively. The minimum will occur for an ignition delay and burn duration of 17 and 55 CA, respectively.

A scatter plot of the nitric oxide concentration for a sample of 1,000 runs is presented in Figure 6-9. The maximum and minimum NO formation was found to be 3,871 ppm and 2,501 ppm, respectively. This resulted in a fluctuation of NO concentration by as much as 23% from the mean cycle NO. The average NO concentration resulting from ccv was found to be 3,248 ppm, which is practically the same as the mean cycle NO. This result supports the conclusion that individual or combined effects of random variations of burn duration and ignition delay have minimal or no affect on the overall nitric oxide emissions. The reason why the overall NO formation does not vary much is due to the fact that NO varies linearly with respect to burn duration and ignition delay. Variations about the mean result in an increase and decrease of NO which for an evenly distributed input data balance each other out.

The average NO concentration as a function of the number of simulation runs is presented in Figure 6-10. The average NO resulting from ccv was calculated for the first 10 runs, 20, etc., up to 1,000 runs. It is evident from the results that the variation of the average NO decreased with increased number of runs. It was found that the average NO after 300 runs varied less than 0.5% and was within 5 ppm of the mean cycle NO after 600 runs. Since each simulation run represents a cycle, the length of time to complete 600 cycles at 1400 rpm would be about 51 seconds. This is a relatively short period of time. As a result, the variations of NO due to random variations of burn duration and ignition delay can be neglected; and the mean cycle simulation could be used to accurately calculate the overall nitric oxide emissions.

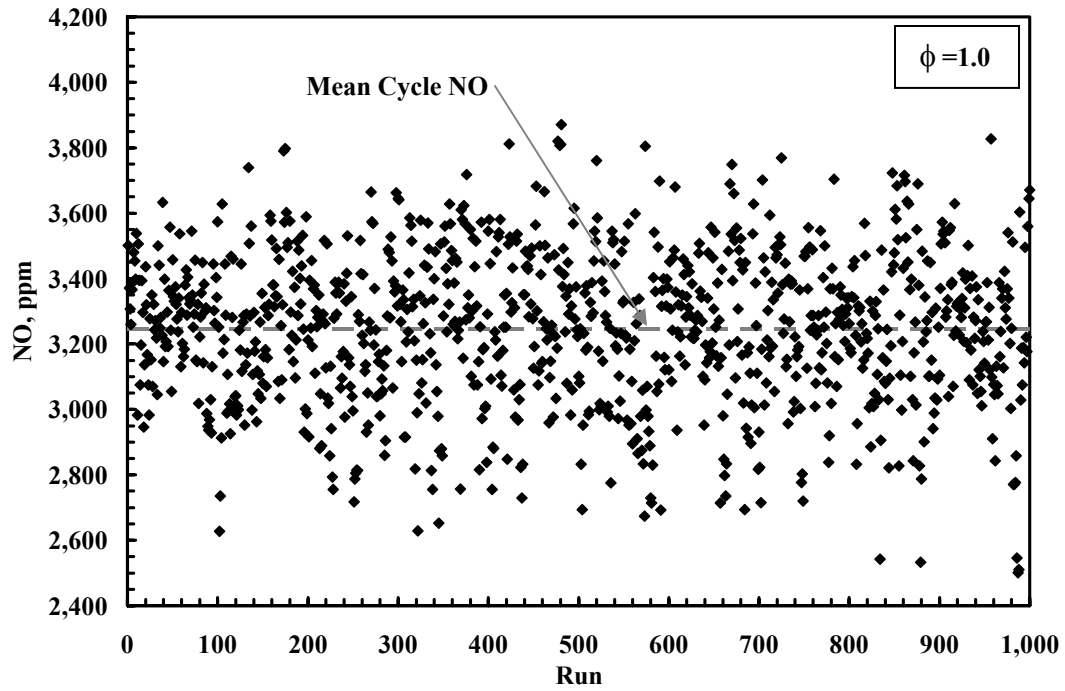


Fig. 6-9. Distribution of NO resulting from random variations of burn duration and ignition delay.

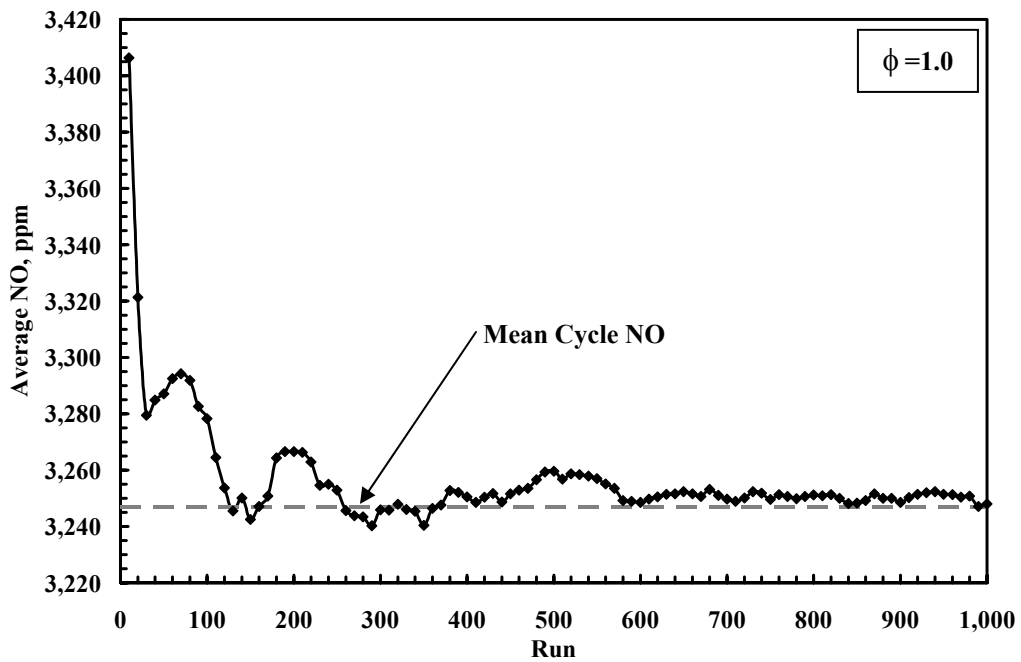


Fig. 6-10. Average NO emissions as a function of simulation runs resulting from variations of burn duration and ignition delay.

Figure 6-11 shows the frequency distribution of the NO concentration for the 1,000 runs. The histogram was created by breaking the range of NO formation into 32 equal intervals of 50 ppm. For each interval the number observations in that interval was counted where the midpoint of the interval is shown on the horizontal axes. The result shows that the frequency distribution of NO is bell shaped which is typical of most normal distribution curves. Therefore, it would be reasonable to assume that variations of NO resulting from random variations of burn duration and ignition delay follow a normal distribution. A normal frequency curve that fits the measured data quite well is for an average NO value of 3,250 ppm with a standard deviation of 210 ppm. The resulting distribution curve is also shown in Figure 6-11.

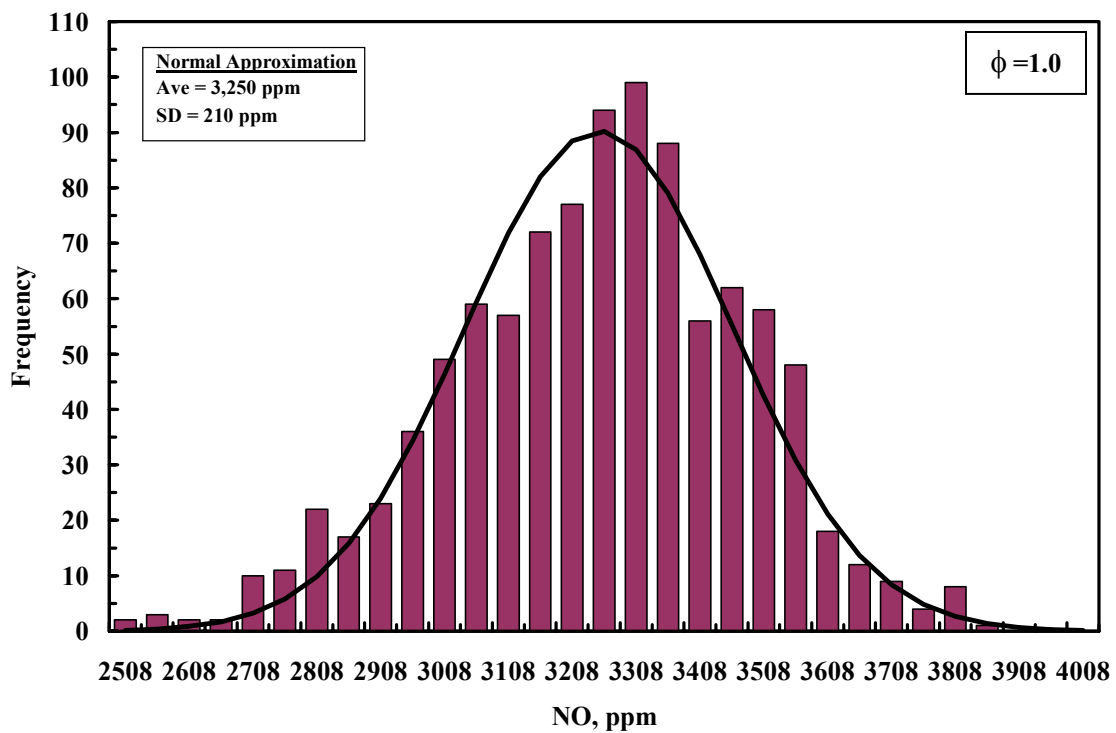


Fig. 6-11. Frequency distribution of NO resulting from 1,000 random variations of burn duration and ignition delay.

6.3.2 Effect of Burn Duration, Ignition Delay and Equivalence Ratio on NO Formation

The effect of varying the combustion duration, ignition delay and equivalence ratio simultaneously will now be examined. A scatter plot of the nitric oxide concentration for a sample of 500 runs is presented in Figure 6-12. The maximum and minimum NO formation that results from varying all three input parameters is 4,774 ppm and 1,193 ppm, respectively. This results in a fluctuation of NO by as much as 47% from the mean cycle NO. The average NO concentration was found to be 3,087 ppm, which is 4.9% less than the mean cycle NO.

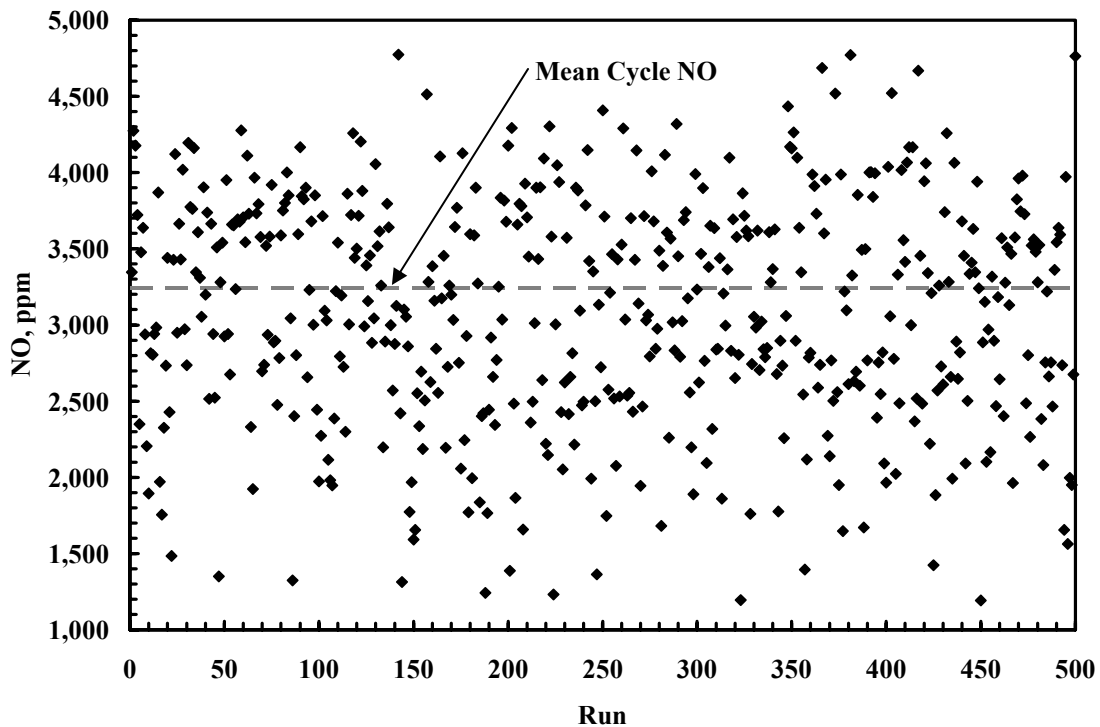


Fig. 6-12. Distribution of NO resulting from random variations of burn duration, ignition delay and equivalence ratio.

The reduction in NO formation is very similar to the case where only the equivalence ratio was randomly varied. This supports the conclusion that variations of burn duration and ignition delay have almost no effect on the overall NO formation. Although cyclic variations of the equivalence ratio seem favorable in terms of reducing the overall NO

emissions, it has a negative impact on the specific fuel consumption. As shown in Figure 6-13, the brake specific fuel consumption (bsfc) is a minimum for slightly lean mixtures ($\phi \sim .98$) and any variation of the equivalence ratio would certainly increase the bsfc. The mean cycle bsfc was found to be 317.2 g/kW-hr. The cyclic variations of all three input parameters resulted in an increase of the average bsfc by 5.8 g/kW-hr or 2%. Variations of the burn duration and ignition delay increased the average bsfc by only 0.75 g/kW-hr. Therefore, it is beneficial to maintain variations of equivalence ratio to a minimum.

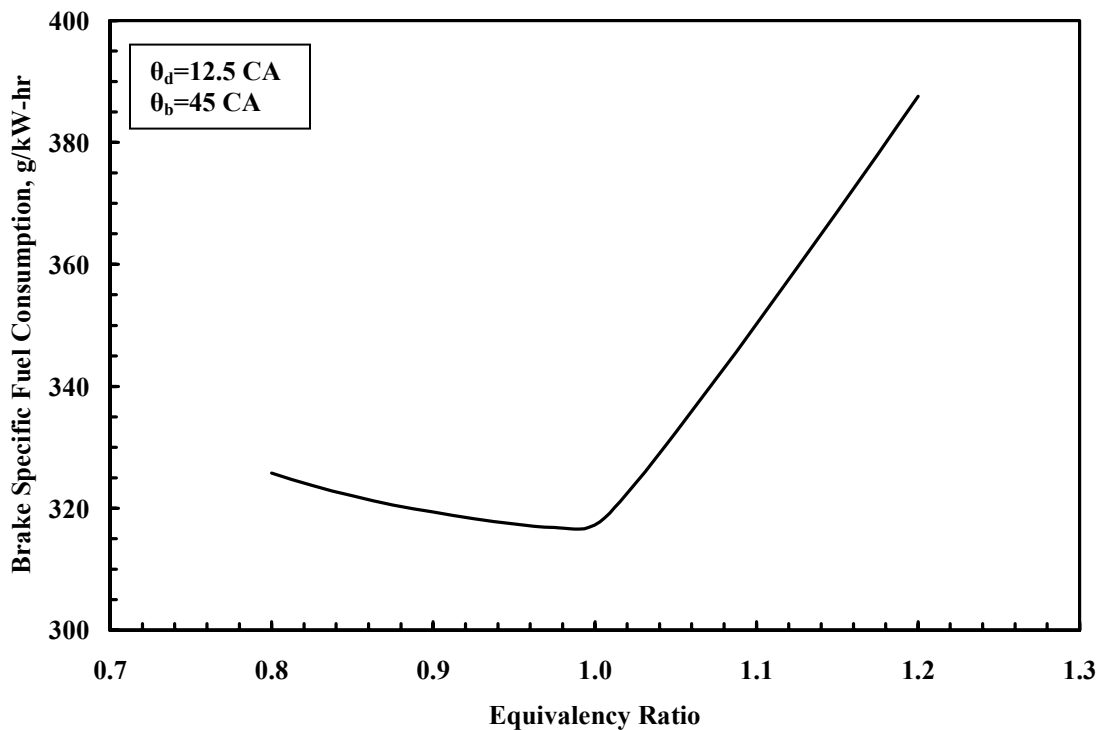


Fig. 6-13. Effect of equivalence ratio on brake specific fuel consumption.

The average NO concentration as a function of the number of simulation runs is presented in Figure 6-14. The variation of the average NO varied less than 0.5% after 300 simulation runs. As a result it would take approximately 26 seconds to reach a nearly steady average NO. Again, this is a relatively short period of time. But, as

mentioned before, the average NO is less than the mean cycle NO by 160 ppm or 4.9%. In this case, ccv of the input parameters should be put into consideration. Since the average NO remains fairly constant after a large number of runs, a simple calibration of the mean cycle model would yield accurate results.

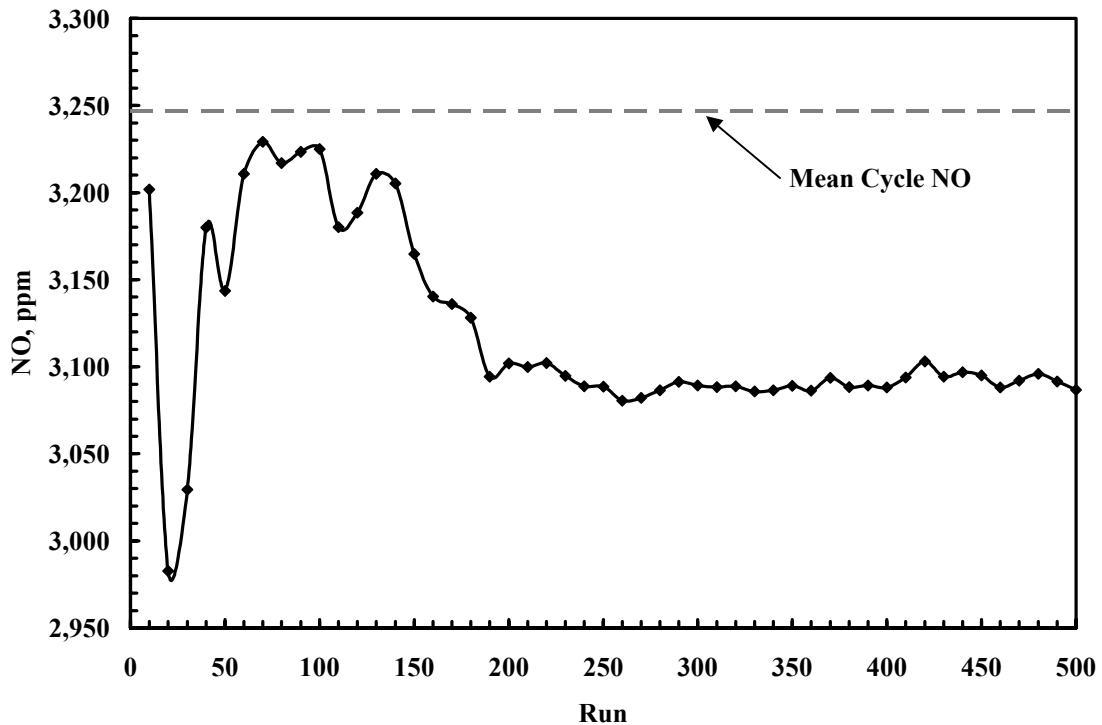


Fig. 6-14. Average NO emissions as a function of simulation runs resulting from the simultaneous variations of all three input parameters.

The frequency distribution of the NO resulting from variations of all three input parameters is shown in Figure 6-15. The frequency distribution of NO does not seem to follow that of a normal distribution. There is a slight dip in the center of the distribution which is not common in normal distributions. This is as a result of the effect that equivalence ratio has on NO formation, which is not linear as compared to burn duration and ignition delay.

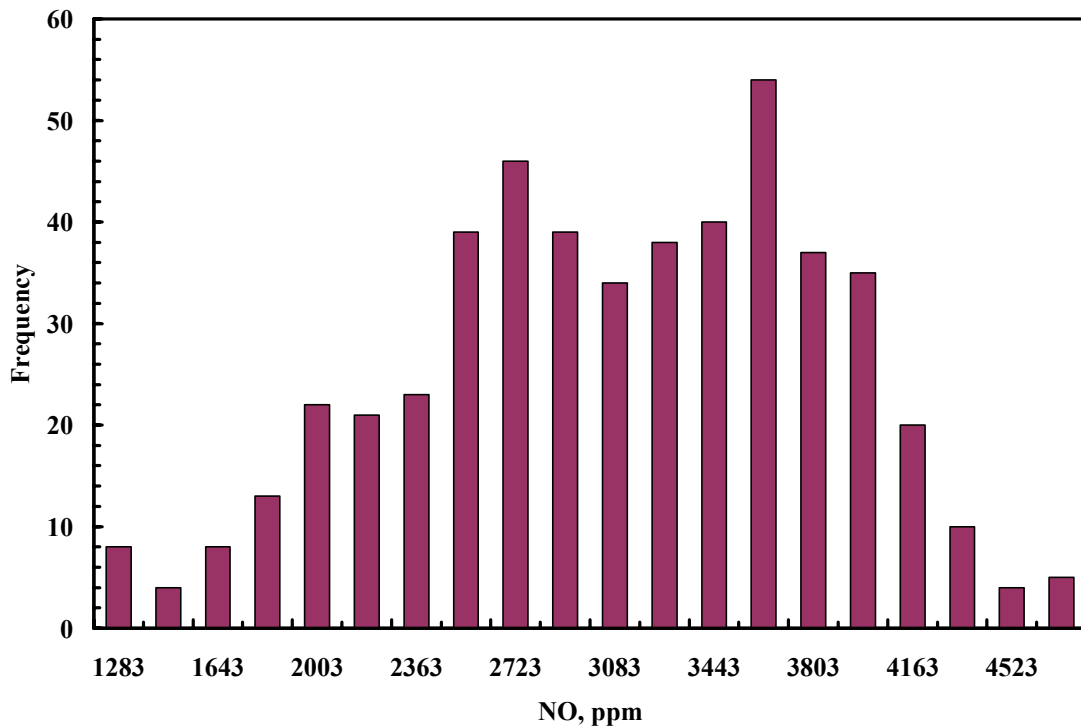


Fig. 6-15. Frequency distribution of NO resulting from random variations of burn duration, ignition delay and equivalence ratio.

6.4 Coefficient of Variance of the Engine Performance Parameters

Calculating the coefficient of variance (COV) of the input and performance parameters can measure the variability of that parameter with respect to its mean. The COV is also a good indicator of the sensitivity of a parameter to changes. The coefficient of variance is defined as

$$\text{COV} = \frac{\sigma}{\mu} \times 100\% \quad (6-1)$$

where σ is the standard deviation and μ is the mean.

The COV for the burn duration, ignition delay and equivalence ratio for all cases studied stayed about the same with a calculated value of 7.7%, 12.0% and 4.1%, respectively.

Table 6-1 shows a summary of the COV for the performance parameters resulting from individual variations. In general, IMEP, bsfc and peak temperature show little sensitivity to variations of burn duration and ignition delay since their COV is relatively small. On the other hand, nitric oxide and peak temperature are highly sensitive to variations of equivalence ratio. Also, NO is slightly sensitive to variations of ignition delay and moderately sensitive to variations of burn duration.

Table 6-1

COV of the engine performance parameters due to individual variations of the input parameters

| | Ignition Delay (%) | Burn Duration (%) | Equivalence Ratio (%) |
|-------------------------|---------------------------|--------------------------|------------------------------|
| IMEP | 0.17 | 0.18 | 2.08 |
| P_{peak} | 3.22 | 5.36 | 1.26 |
| θ_{pp} | 7.5 | 9.22 | 1.14 |
| NO | 3.65 | 6.25 | 21.92 |
| bsfc | 0.20 | 0.22 | 2.30 |
| T_{peak} | 0.27 | 1.05 | 14.55 |

The COV for the various engine performance parameters resulting from variations of two input parameters (burn duration and ignition delay) and three input parameters (burn duration, ignition delay and equivalence ratio) is presented in Figure 6-16. Comparing the COV for both cases shows that the COV of peak pressure, angle of peak pressure and peak temperature do not vary much. On the other hand, the COV of IMEP, NO and bsfc increased significantly. The cyclic variability for IMEP and bsfc increased more than 600% as a result of including variations of equivalence ratio. The increased variation of bsfc caused an increase in the specific fuel consumption. The COV of IMEP is considered to be an important factor in determining engine stability. Ferguson and Kirkpatrick [5] reported that the COV of IMEP for an engine should be kept below 10% to run smoothly. For the individual and combined variations, the COV of IMEP is below the limit and the engine should run fairly smoothly.

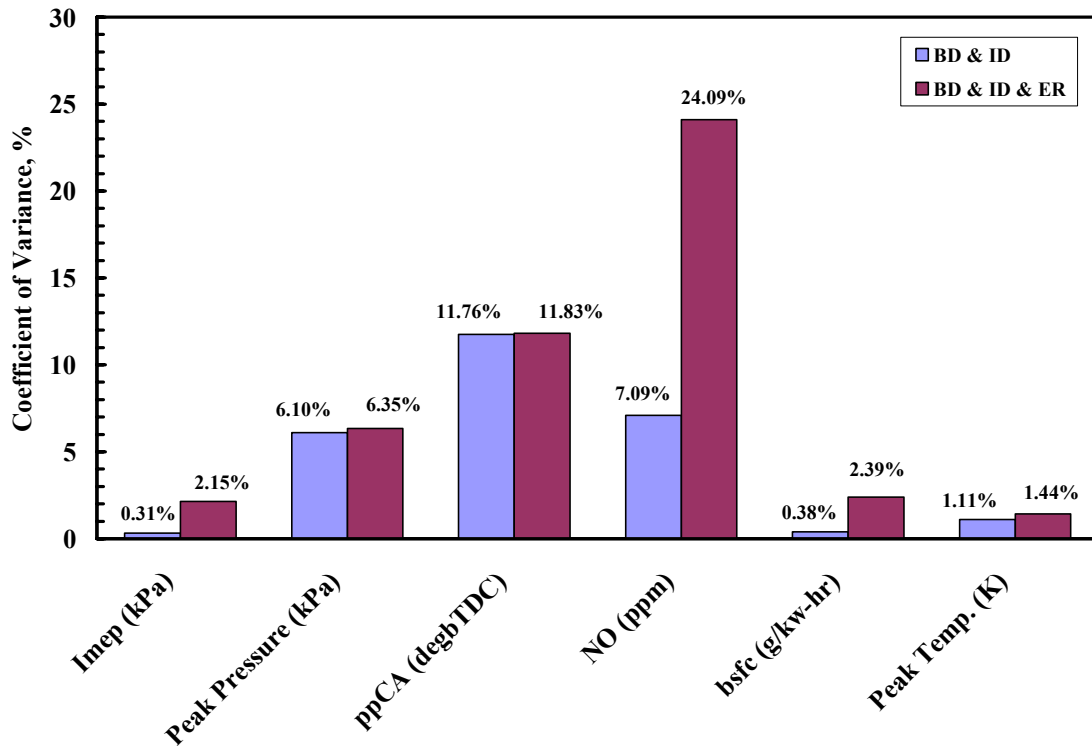


Fig. 6-16. Coefficient of variance for engine performance parameters.

From Figure 6-16, the COV of NO increased from 7.09% to 24.09%, an increase of more than 300%. The increased variation caused the decrease in the average NO emissions. Furthermore, it can be said that small increases in peak temperature variations cause relatively large variations of NO concentration. From the results, an increase in COV of the peak temperature from 1.11% to 1.44%, an increase of 0.33%, caused the COV of NO to more than triple. This supports the belief that NO is strongly effected by the burned gas temperature.

6.5 Data Validation

The simulation mean and standard deviation of the cylinder peak pressures, crank angle of peak pressure and IMEPs were compared to those acquired experimentally by Brehob and Newman [3]. The experimental and simulation results are shown in Table 6-2. The simulation average values of all three performance parameters are similar to those found

experimentally. The greatest difference was between the average IMEPs, which resulted in the simulation value being 3% less than the experimental value. On the other hand, the standard deviation of the IMEPs differed greatly. The standard deviation from the simulation was more than twice the standard deviation acquired experimentally. The large difference might be due to the fact that the simulation only considered the variations of only three parameters (combustion duration, ignition delay and equivalence ratio) whereas the results for the experiments reflect variations of many additional parameters. The simulation standard deviation of the other two parameters was within 10% of the experimental value.

Table 6-2

Comparison of the mean and standard deviation of experimental data of Brehob and Newman [3] with that of the current simulation

| Item | Experiment | | Simulation | |
|---------------|------------|--------------------|------------|--------------------|
| | Mean Value | Standard Deviation | Mean Value | Standard Deviation |
| P_{Peak} | 21.0 bar | 1.47 bar | 21.0 bar | 1.33 bar |
| θ_{pp} | 16.3 aTDC | 1.91 CA | 16.6 aTDC | 1.97 CA |
| IMEP | 4.12 bar | 0.037 bar | 4.00 bar | 0.086 bar |

CHAPTER VII

SUMMARY AND CONCLUSION

7.1 Summary

Since the nitric oxide formation process is strongly affected by the gas temperature and since cyclic variation will produce cycles with different gas temperatures, the effect of ccv on NO emissions was thought to be potentially important. As a result, a detailed investigation was carried out using an engine simulation capable of modeling NO formation using the extended Zeldovich mechanism. The performance parameters acquired by the simulation show good agreement with experimental data. The results from this study can be summarized as follows:

1. NO emission is roughly linear with respect to either variations of combustion duration or ignition delay, but variation of NO with respect to equivalence ratio is quadratic where the maximum occurs at an equivalence ratio of approximately 0.94.
2. Variations of NO on a cycle by cycle basis were greatest with ccv of equivalence ratio which caused the NO to fluctuate as much as 59% from the mean cycle NO. Varying all three parameters as compared to two parameters (Burn duration and ignition delay) increased the cycle-to-cycle variations of NO from 23% to 47%, due to the strong influence of equivalence ratio on NO.
3. Cyclic variations of combustion duration and ignition delay, individually and simultaneously, yield an average NO that is within 0.5% of the mean cycle NO. Variations of both parameters have no effect on the overall NO formation.

4. Cyclic variations of all three input parameters yield an average NO that is about 5% less than the mean cycle NO, indicating that ccv must be considered to get accurate results.
5. The COV of the input and performance parameters shows that NO formation is highly sensitive to variation of equivalence ratio and temperature.

7.2 Conclusion

Although NO varies greatly from cycle to cycle, results from this study show that the variation of the average NO is small after a short period of time. This result allows us to calibrate the mean cycle model thereby incorporating the effects of ccv. Simulations can then be carried out at a faster pace and with accurate results. For other conditions and other variables, this conclusion may not be valid. A similar study must be carried out to determine a relationship between the mean cycle and the magnitude of cyclic variations.

REFERENCES

1. Ramos, J. I., in *Computer Simulation for Fluid Flow, Heat and Mass Transfer, and Combustion in Reciprocating Engines*, (N. C. Markatos, Ed.). Hemisphere Publishing Corporation, New York, pp 21-65, 1989.
2. Young, M. B., *SAE Paper 810020* (1981).
3. Brehob, D. D., and Newman, C. E., *SAE Paper 922165* (1992).
4. Ozdor, N., Dulger, M., and Sher, E., *SAE Paper 940987* (1994).
5. Ferguson, C. R., and Kirkpatrick, A. T., *Internal Combustion Engines: Applied Thermosciences* (2nd Ed.). John Wiley & Sons Inc., New York, 2001.
6. Stone, R., *Introduction to Internal Combustion Engines* (3rd Ed.). S. A. E., Warrendale, Pa., 1999, ISBN 0-7680-0495-0.
7. Weaver, C. E., and Santavicca, D. A., *SAE Paper 922171* (1992).
8. Starkman, E. S., Strange, S. F., and Dahm, T. J., *SAE Paper 83V* (1959).
9. Ho, C. M., and Santavicca, D. A., *SAE Paper 872100* (1987).
10. Winsor, R. E., Patterson, D. J., *SAE Paper 730086* (1973).
11. Barton, R. K., Kenemuth, D. K., Lestz, S. S., and Meyer, W. E., *SAE Paper 700488* (1970).
12. Bates, S. C., *SAE Paper 892086* (1989).
13. Heywood, J. B., and Vilchis, F. R., *Comb. Sci. Tech.* 38;313 (1984).
14. Lucas, G. G., and Brunt, M. F. J., *SAE Paper 820165* (1982).
15. Poulus, S. G., and Heywood, J. B., *SAE Paper 830334* (1983).
16. Caton, J. A., "Detailed Results for Nitric Oxide Emissions as Determined From a Multiple-Zone Cycle for a Spark-Ignition Engine," ICE-Vol-39, Paper No. ICEF2002-491, pp 131-148, *Proceedings of the 2002 Fall Technical Conference of the American Society of Mechanical Engineers*, New Orleans, LA, 08-11 September 2002.

17. Caton, J. A., "A Multi-Zone Cycle Simulation for Spark-Ignition Engines: Thermodynamic Details," ICE-Vol-37-2, Paper No. 2001-ICE-412, pp 41-58, *Proceedings of the 2001 Fall Technical Conference American Society of Mechanical Engineers*, Argonne, IL, 23-26 September 2001.
18. Caton, J. A., in *Modeling of SI Engines and Multi-Dimensional Engine Modeling*, S. A. E., Warrendale, PA, pp 65-83, 2002.
19. Caton, J. A., "Extension of a Thermodynamic Cycle Simulation to Include Computations of Nitric Oxide Emissions for Spark-Ignition Engines," Report No. ERL-2002-01, Version 1.0, Engine Research Laboratory, Department of Mechanical Engineering, Texas A&M University, 22 July 2002.
20. Annamalai, K., and Puri, I. K., *Combustion Engineering*, CRC Press, New York, (in press).
21. Ramos, J. I., *Internal Combustion Engine Modeling*. Hemisphere Publishing Corporation, New York, 1989.
22. Caton, J. A., "The Use of a Three-Zone Combustion Model to Determine Nitric Oxide Emissions From a Homogeneous-Charge, Spark-Ignited Engine," Paper No. ICES2003-598, *Proceedings of the 2003 Spring Technical Conference of the American Society of Mechanical Engineers*, Salzburg, Austria, 11-14 May 2003.
23. Dean, A. M., and Bozzelli, J. W., in *Gas-Phase Combustion Chemistry*, (W. C. Gardiner, Ed.). Springer-Verlag, New York, pp 125-342, 2000.
24. Caton, J. A., "A Thermodynamic Cycle Simulation for Spark-Ignition Engines Including the Second Law of Thermodynamics Using Multiple Zones for Combustion," Report No. ERL-2001-01, Version 1.0, Engine Research Laboratory, Department of Mechanical Engineering, Texas A&M University, 22 June 2001.

APPENDIX A
OTHER VARIABLES AFFECTING NITRIC OXIDE FORMATION

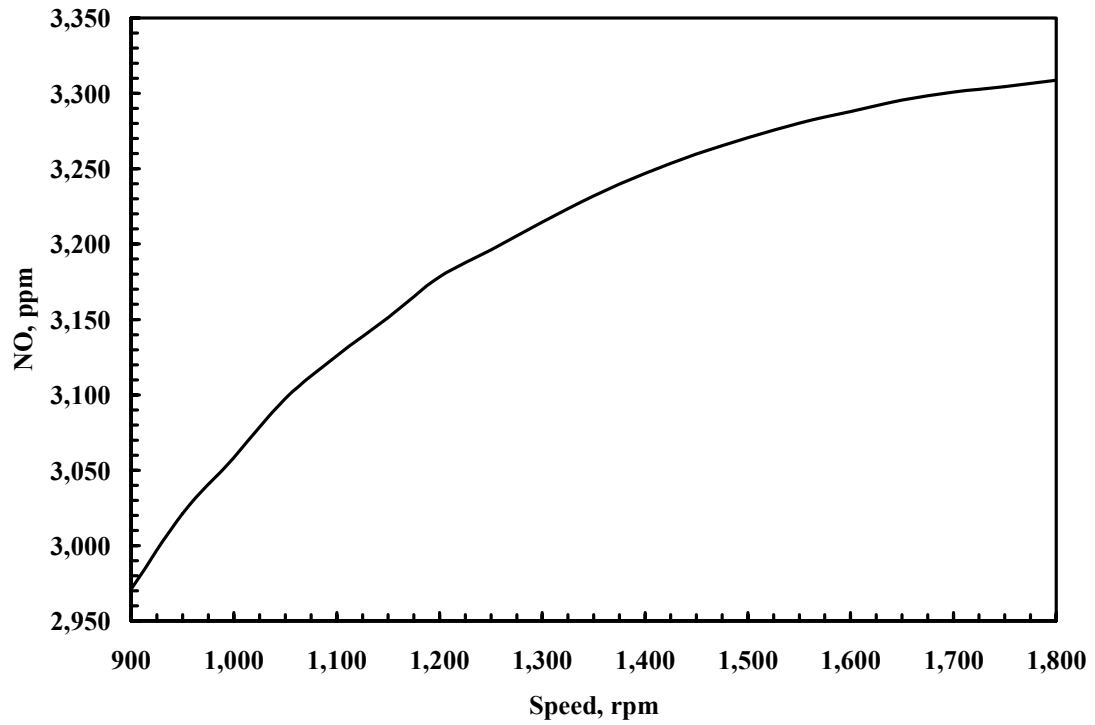


Fig. A-1. The effect of engine speed on NO formation.

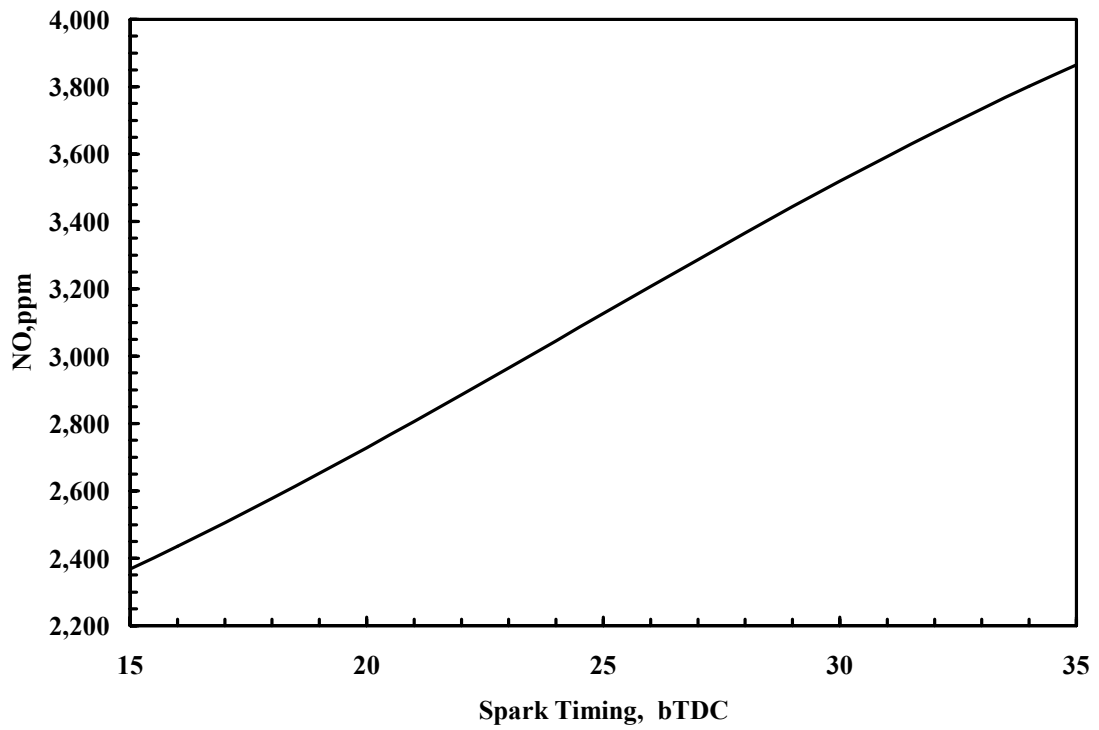


Fig. A-2. The effect of spark timing on NO formation.

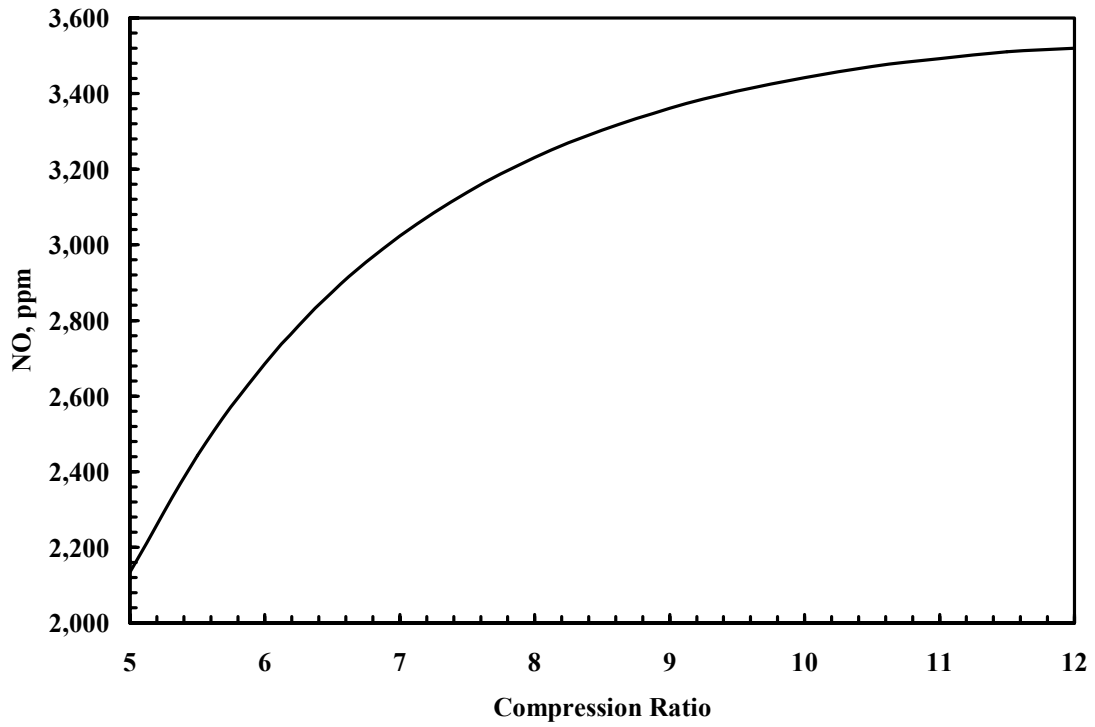


Fig. A-3. The effect of compression ratio on NO formation.

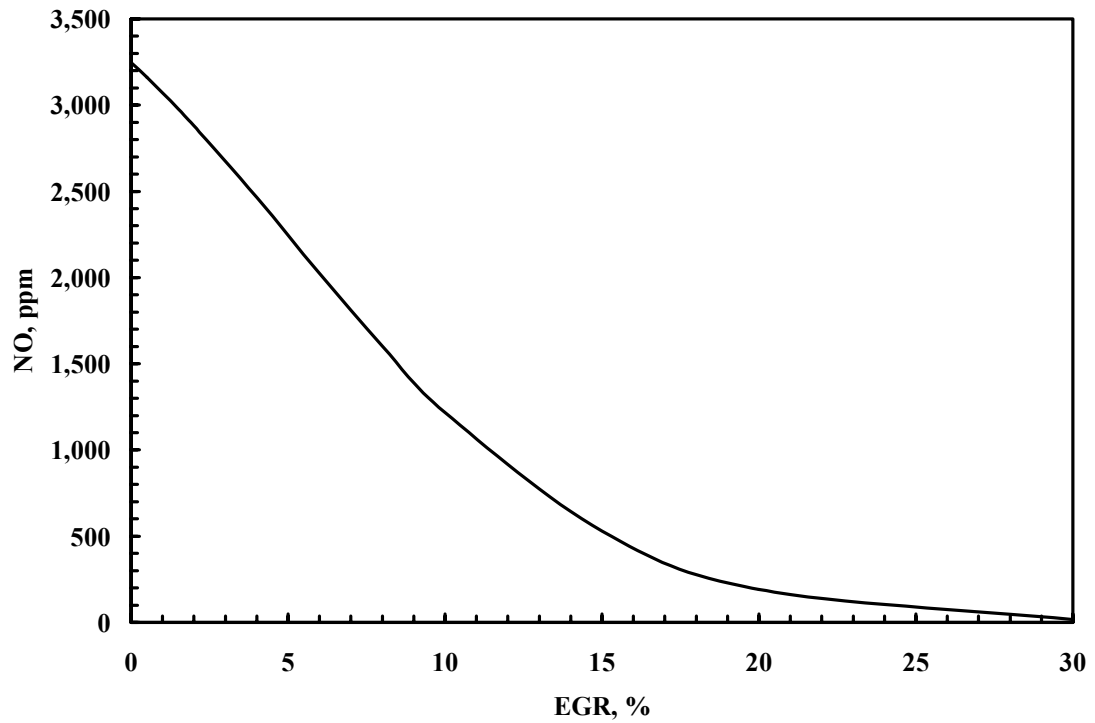


Fig. A-4. The effect of exhaust gas residual (EGR) on NO formation.

VITA

Name: Milivoy Villarroel

Permanent Address: 3212 Hallran Road
Falls Church, VA 22041

Phone: (703) 820-4021

Email: mvillarr@tamu.edu

Education: M.S., Mechanical Engineering, August 2004
Texas A&M University
College Station, TX.
B.S., Mechanical Engineering, May 2002
Virginia Polytechnic Institute and State University
Blacksburg, VA

Work Experience: Burt Hill Kosar Rittelmann Associates (Summer 2003)
Washington, DC
Ford Motor Company (Summer 2000)
Dearborn, MI
General Motors Corporation (Summer 1999)
Baltimore, MD
Cox Communications (November 1997 – January 1999)
Virginia Beach, VA